Atmos. Chem. Phys., 20, 11089–11117, 2020
https://doi.org/10.5194/acp-20-11089-2020

Atmospheric Chemistry and Physics
Open Access
EGU

The ice-nucleating activity of Arctic sea surface microlayer samples and marine algal cultures

Luisa Ickes[1,2,a], Grace C. E. Porter[3], Robert Wagner[2], Michael P. Adams[3], Sascha Bierbauer[2], Allan K. Bertram[4], Merete Bilde[5], Sigurd Christiansen[5], Annica M. L. Ekman[1], Elena Gorokhova[6], Kristina Höhler[2], Alexei A. Kiselev[2], Caroline Leck[1], Ottmar Möhler[2], Benjamin J. Murray[3], Thea Schiebel[2], Romy Ullrich[2], and Matthew E. Salter[6]

[1]Department of Meteorology, Bolin Centre for Climate Studies, Stockholm University, Stockholm, Sweden
[2]Institute of Meteorology and Climate Research, Karlsruhe Institute of Technology, Karlsruhe, Germany
[3]School of Earth and Environment, University of Leeds, Leeds, United Kingdom
[4]Department of Chemistry, University of British Columbia, Vancouver, Canada
[5]Department of Chemistry, Aarhus University, Aarhus, Denmark
[6]Department of Environmental Science and Analytical Chemistry, Bolin Centre for Climate Studies, Stockholm University, Stockholm, Sweden
[a]now at: Department of Space, Earth and Environment, Chalmers, Gothenburg, Sweden

Correspondence: Luisa Ickes (luisa.ickes@misu.su.se)

Received: 12 March 2020 – Discussion started: 24 March 2020
Revised: 16 July 2020 – Accepted: 22 July 2020 – Published: 29 September 2020

Abstract. In recent years, sea spray as well as the biological material it contains has received increased attention as a source of ice-nucleating particles (INPs). Such INPs may play a role in remote marine regions, where other sources of INPs are scarce or absent. In the Arctic, these INPs can influence water–ice partitioning in low-level clouds and thereby the cloud lifetime, with consequences for the surface energy budget, sea ice formation and melt, and climate. Marine aerosol is of a diverse nature, so identifying sources of INPs is challenging. One fraction of marine bioaerosol (phytoplankton and their exudates) has been a particular focus of marine INP research. In our study we attempt to address three main questions. Firstly, we compare the ice-nucleating ability of two common phytoplankton species with Arctic seawater microlayer samples using the same instrumentation to see if these phytoplankton species produce ice-nucleating material with sufficient activity to account for the ice nucleation observed in Arctic microlayer samples. We present the first measurements of the ice-nucleating ability of two predominant phytoplankton species: *Melosira arctica*, a common Arctic diatom species, and *Skeletonema marinoi*, a ubiquitous diatom species across oceans worldwide. To determine the potential effect of nutrient conditions and characteristics of the algal culture, such as the amount of organic carbon associated with algal cells, on the ice nucleation activity, *Skeletonema marinoi* was grown under different nutrient regimes. From comparison of the ice nucleation data of the algal cultures to those obtained from a range of sea surface microlayer (SML) samples obtained during three different field expeditions to the Arctic (ACCACIA, NETCARE, and ASCOS), we found that they were not as ice active as the investigated microlayer samples, although these diatoms do produce ice-nucleating material. Secondly, to improve our understanding of local Arctic marine sources as atmospheric INPs we applied two aerosolization techniques to analyse the ice-nucleating ability of aerosolized microlayer and algal samples. The aerosols were generated either by direct nebulization of the undiluted bulk solutions or by the addition of the samples to a sea spray simulation chamber filled with artificial seawater. The latter method generates aerosol particles using a plunging jet to mimic the process of oceanic wave breaking. We observed that the aerosols produced using this approach can be ice active, indicating that the ice-nucleating material in seawater can indeed transfer to the aerosol phase. Thirdly, we attempted to measure ice nucleation activity across the entire temperature range relevant for mixed-phase clouds using a suite of ice nucleation measurement techniques – an expansion cloud chamber, a

continuous-flow diffusion chamber, and a cold stage. In order to compare the measurements made using the different instruments, we have normalized the data in relation to the mass of salt present in the nascent sea spray aerosol. At temperatures above 248 K some of the SML samples were very effective at nucleating ice, but there was substantial variability between the different samples. In contrast, there was much less variability between samples below 248 K. We discuss our results in the context of aerosol–cloud interactions in the Arctic with a focus on furthering our understanding of which INP types may be important in the Arctic atmosphere.

1 Introduction

Clouds have a strong impact on the energy balance and therefore play an important role in the Earth's climate system (Chahine, 1992; Boucher et al., 2013). They are particularly important in the high latitudes, which is one of the regions most sensitive to global warming (Stocker et al., 2013), where they not only influence the energy budget (Garrett et al., 2009; Morrison et al., 2012) but also the subsequent melting and freezing of sea ice (Intrieri et al., 2002; Pithan and Mauritsen, 2014). As such, they are involved in several climate feedback processes. The radiative characteristics of clouds depend on their microphysical structure, e.g. whether the cloud consists of water droplets or ice crystals. Mixed-phase clouds which are comprised of both ice crystals and super-cooled water droplets are common in the high Arctic (Shupe et al., 2006). Formation of liquid cloud droplets requires the presence of aerosol particles that facilitate water vapour condensation on its surface (so-called cloud condensation nuclei – CCN). Aerosol particles are also necessary for the initiation of primary ice formation within these clouds by a process known as heterogeneous freezing (so-called ice-nucleating particles – INPs). Typically, only a small fraction of aerosol particles has the ability to nucleate ice. Despite increasing interest in INPs (Szyrmer and Zawadzki, 1997; Hoose and Möhler, 2012; DeMott et al., 2010), it is still uncertain which types of aerosol particles constitute good INPs in the atmosphere (Kanji et al., 2017). Aerosol particles known to nucleate ice crystals by heterogeneous freezing in mixed-phase clouds include mineral dust, volcanic ash, and primary biological particles, such as pollen, fungi, and bacteria as well as their fragments (Hoose and Möhler, 2012). Those are aerosol particles with a predominantly terrestrial source. However, there are regions which are relatively isolated from terrestrial sources, such as the summer high Arctic and remote parts of the North Atlantic, North Pacific, and Southern Ocean. In such regions, sea spray aerosol could be an important source of INP (Burrows et al., 2013; Yun and Penner, 2013; Vergara-Temprado et al., 2017; Huang et al., 2018; McCluskey et al., 2018a, b; Creamean et al., 2019).

The potential for marine environments to act as sources of INPs was first investigated during the 1960s (see Table 1). This area of research has attracted renewed attention in more recent years. Indeed, recent observations indicate that biogenic material present at the interface between the ocean and atmosphere, the so-called sea surface microlayer (SML), and within nascent sea spray aerosol can be ice active (e.g. Knopf et al., 2011; Wilson et al., 2015; DeMott et al., 2016; Irish et al., 2017; and Gong et al., 2020). Previous studies can be separated into three main groups: (i) ambient ice nucleation measurements in marine environments, (ii) studies investigating the ice-nucleating potential of seawater and SML samples, and (iii) studies concerned with the ice-nucleating potential of different phytoplankton species and their exudates (Table 1). One of the key recent studies concerned with whether sea spray aerosol contains significant concentrations of INPs was conducted by DeMott et al. (2016), who examined the ice nucleation potential of laboratory-generated nascent sea spray aerosol particles and compared their findings with measurements of ambient marine aerosol. Critically, they observed that laboratory-generated sea spray aerosol has a similar ice nucleation activity to ambient marine aerosols and that the ice-nucleating activity of nascent sea spray aerosol strongly increased in association with phytoplankton blooms. Given these observations, the authors conclude that the INPs present in sea spray aerosol are likely linked to organic matter associated with phytoplankton blooms. DeMott et al. (2016) also showed that different INP types were active at different temperatures. Despite the finding that significant amounts of ice-active material are present in nascent sea spray aerosol, the measured number concentration of INPs in ambient marine aerosol was still several orders of magnitude lower than equivalent measurements in ambient terrestrial aerosol. Another relevant study was conducted by Wilson et al. (2015), who analysed SML samples collected in the Atlantic and Arctic oceans. The ice activity of these samples was highly variable with the temperature at which half of the sample droplets froze, the so-called median freezing temperature, ranging from approximately 265 to 248 K. Based on tests with samples that have been filtered and heated, these authors concluded that submicron biogenic material was likely responsible for the ice activity of seawater samples from a range of locations. This suggests that whole cells are not responsible for the observed ice nucleation (Schnell and Vali, 1975; Wilson et al., 2015; Irish et al., 2017). Further, exudates of the marine diatom *Thalassiosira pseudonana*, a widespread phytoplankton species, have been shown to nucleate ice (Knopf et al., 2011; Wilson et al., 2015; Ladino et al., 2016); hence, it has been proposed that organic material associated with phytoplankton cell exudates may explain the ice nucleation activity of marine SML samples. However, Knopf et al. (2011) also found that intact cells are effective INPs in the mixed-phase temperature regime. Another hypothesis is that bacteria play a role as shown by, for example, Fall and Schnell (1985).

Motivated by these previous studies, we have analysed the freezing potential of two common phytoplankton species: *Melosira arctica* (MA) and *Skeletonema marinoi* (SM). *Skeletonema marinoi* is a very common diatom species, especially in temperate coastal regions during the spring bloom (Kooistra et al., 2008). *Melosira arctica*, on the other hand, is the most productive algae in the Arctic Ocean (Booth and Horner, 1997). *Melosira arctica* was found along with polymer gels in high-Arctic cloud water samples (Orellana et al., 2011). Environmental factors, such as light and nutrient supply, have a high potential to affect the biochemical composition of phytoplankton and thus biogenic exudate material. The degree to which both the flux and composition of sea spray aerosol is affected by biological activity in the surface ocean is a long-standing question in the field. However, studies have suggested that the aerosol flux may not only be impacted by the absolute cell concentrations of phytoplankton but also by their growing conditions (e.g. Alpert et al., 2015). Thus those environmental factors have an effect on the presence of INPs coming from marine sources as well. Therefore, algae grown under different nutrient regimes may differ in their INP ability, which is investigated in this study. *Skeletonema marinoi* was cultivated with different nutrition levels in order to mimic nutrient limitation and growth inhibition in phytoplankton. This leads to a variation in the carbon contents of each cell and thus in the cell suspensions, which enables us to investigate the resulting effects of different growth rates and cell carbon content on ice nucleation. Our aim was to investigate whether changing these cell properties has any impact on the ice nucleation activity of the phytoplankton.

Another goal of this study was to improve our understanding of whether Arctic marine regions may have local sources of marine INPs. Although it has been found that organic matter with marine origin is prevalent in aerosol particles present in the high Arctic during summer (e.g. Leck et al., 2002) and that marine organic matter nucleates ice (e.g. Wilson et al., 2015), the ice-nucleating potential of the aerosolized organic matter has not been examined in detail for the Arctic region. Therefore, we have determined the heterogeneous ice-nucleating ability of artificial seawater containing two phytoplankton species cultured in the laboratory along with samples of SML collected during a series of field campaigns in the North Atlantic and Arctic Ocean. Within this study, two different aerosolization techniques were utilized to test the impact of the aerosol generation method on the ice nucleation behaviour of the resulting particles.

Measurements have been made with a variety of ice nucleation measurement techniques, and all measurements were conducted under conditions relevant for mixed-phase clouds, i.e. above about 235 K and at water saturation. We have utilized a number of different experimental methods to derive the ice-nucleating ability of our samples, with the ultimate goal of merging these different measurements across the full temperature range relevant for mixed-phase clouds. Through comparison of the ice nucleation activity of artificial seawater containing *Melosira arctica* with that of the SML samples, we aim to shed light on how representative relevant algal cultures are for Arctic marine INP.

A description of the methods of sample collection and cultivation as well as the experimental setup and ice nucleation measurement techniques is introduced in Sect. 2. The results of the ice nucleation measurements and a comparison with previous marine INP measurements found in the literature are presented in Sect. 3. Since we have made measurements across the full temperature range relevant for mixed-phase clouds (273.15 until 233.15 K), this section is split into three parts. The first part (Sect. 3.1) focuses on the measurements at temperatures above 248 K, referred to as the "high-temperature regime" throughout this article, while the second part (Sect. 3.2) focuses on the measurements conducted at temperatures below 248 K, referred to as the "low-temperature regime" throughout this article. In the final part (Sect. 3.3), we present an integrated spectrum over the full temperature range. Finally, we conclude this study with a summary of the major findings and discussion of potential atmospheric implications of our results (Sect. 4).

2 Methods and experimental setup

To determine the ice-nucleating ability of our samples, we have used three independent methods (Fig. 1). Firstly, bulk cell suspensions of the algal cultures and field samples were aerosolized using a nebulizer and the generated particles were injected into the Aerosol Interaction and Dynamics in the Atmosphere (AIDA) aerosol and cloud chamber (Möhler et al., 2008). The ice nucleation behaviour of the particles was then either measured in situ in the AIDA chamber by performing an expansion-cooling experiment or by probing the particles with a continuous-flow diffusion chamber (CFDC) called INKA (Ice Nucleation instrument of the KArlsruhe Institute of Technology; Schiebel, 2017). Secondly, for a subset of the samples, a certain volume of the bulk solutions was added to 20 L of artificial seawater in the mobile Aarhus University sea spray simulation chamber called AEGOR (Christiansen et al., 2019). Aerosol particles generated by bubble bursting in AEGOR were injected into the AIDA chamber in the same manner as the particles generated using the nebulizer, and their ice nucleation activity was measured in both the AIDA expansion-cooling experiment and with INKA. Thirdly, the INP abundance within the liquid samples used to generate aerosols was determined using the microlitre nucleation by immersed particle instrument (µl-NIPI), where droplets of the bulk solutions were pipetted onto a cold stage (Whale et al., 2015).

Additionally, it was investigated if material from the same algal cultures and SML samples affects the ability of sea spray aerosols to act as CCN. The measurements of the CCN-derived hygroscopicity and the implication on Arctic clouds

https://doi.org/10.5194/acp-20-11089-2020

Table 1. An overview of previous laboratory and field studies which have either investigated nascent sea spray aerosol particles as INP or ambient INP in marine regions (including SML or seawater samples) in the temperature range of mixed-phase clouds. The location ("Loc.") of each of the field studies is given. Laboratory studies are indicated as "Lab". The "Data" column indicates how the ice nucleation activity was estimated (usual measures are as concentration of $\mathrm{INP\,m^{-3}}$ or $\mathrm{INP\,L^{-1}}$, the frozen fraction (FF) as a function of temperature, or the median freezing temperature T_{50}, i.e. the temperature at which 50 % of the droplets were frozen). Where relevant, the "Subst." column states specific substances or species that were studied. The column "Instr." provides information about the instrument(s) used in the study; different cloud chambers are simplified by the term "Cloud chamber", with reference to the basic principle given in the following index (1: Warner, 1957; 2: Bigg, 1957; 3: Bigg et al., 1963; 4: Langer et al., 1967; 5: Stevenson, 1968; 6: Gagin and Arroyo, 1969; and 7: Langer and Rodgers, 1975). CFDC stands for continuous-flow diffusion chamber. Cold stage, freezing assays, etc., are all described with the term "drop freez.".

(i) Ambient ice nucleation measurements in marine environments

Study	Loc.	Data	Subst.	Instr.
Kline and Brier (1958)	Washington DC	$\mathrm{INP\,L^{-1}}$	Airborne	Cloud chamber[1]
Isono et al. (1959)	Tokyo (Pacific)	$\mathrm{INP\,L^{-1}}$	Airborne	Cloud chamber[2]
Battan and Riley (1960)	Arizona (Gulf of Mexico)	$\mathrm{INP\,L^{-1}}$	Airborne	Cloud chamber[1]
Kline (1960)	Washington DC	$\mathrm{INP\,L^{-1}}$	Airborne	Cloud chamber[1]
Bigg (1973)	Southern Ocean (SO)	$\mathrm{INP\,m^{-3}}$	Airborne	Filter & cloud chamber[6]
Radke et al. (1976)	Alaska	$\mathrm{INP\,L^{-1}}$	Airborne	Filter & dyn. chamber[4]
Schnell (1977)	Canada (Atlantic)	$\mathrm{INP\,m^{-3}}$	Airborne	Filter & drop freez.
Flyger and Heidam (1978)	Northern Greenland	$\mathrm{INP\,L^{-1}}$	Airborne	Filter & cloud chamber[5]
Borys and Grant (1983)	Arctic	$\mathrm{INP\,m^{-3}}$	Airborne	Filter & cloud chamber[5]
Nagamoto et al. (1984)	Florida	$\mathrm{INP\,m^{-3}}$	Airborne	Filter & cloud chamber[7]
Fountain and Ohtake (1985)	Alaska	$\mathrm{INP\,L^{-1}}$	Airborne	Filter & cloud chamber[3]
Rosinski et al. (1986)	Pacific	Freez. T, $\mathrm{INP\,m^{-3}}$	Airborne	Filter & drop freez. & cloud chamber[7]
Rosinski et al. (1987)	Pacific	Freez. T, $\mathrm{INP\,m^{-3}}$	Airborne	Filter & dyn. chamber[7]
Borys (1989)	Arctic	$\mathrm{INP\,m^{-3}}$	Airborne	Filter & cloud chamber[7]
Bigg (1990)	SO, Hawaii	$\mathrm{INP\,m^{-3}}$	Airborne	Filter & cloud chamber[3,5,6]
Rosinski et al. (1995)	East China Sea	$\mathrm{INP\,m^{-3}}$	Airborne	Filter & dyn. chamber[7]
Rosinski (1995)	Washington State (North Pacific)	$\mathrm{INP\,m^{-3}}$	Airborne	Filter & dyn. chamber[7]
Bigg (1996)	Arctic	$\mathrm{INP\,m^{-3}}$	Airborne	Filter & cloud chamber[5]
DeMott et al. (2016)	Caribbean, Arctic, Canada, Pacific, Lab (MART)	$\mathrm{INP\,L^{-1}}$	Airborne	CFDC, filter & drop freez.
Mason et al. (2015)	Canada (North Pacific)	$\mathrm{INP\,L^{-1}}$	Airborne	Filter & drop freez.
Ladino et al. (2016)	Canada (North Pacific)	$\mathrm{INP\,L^{-1}}$	Airborne	CFDC
Creamean et al. (2018)	Arctic	$\mathrm{INP\,L^{-1}}$	Airborne	Filter & drop freez.
McCluskey et al. (2018b)	Mace Head	$\mathrm{INP\,L^{-1}}$	Airborne	CFDC, filter & drop freez.
McCluskey et al. (2018a)	SO	$\mathrm{INP\,m^{-3}}$	Airborne	CFDC, filter & drop freez.
Si et al. (2018)	Canada/Arctic	$\mathrm{INP\,L^{-1}}$	Airborne	Filter & drop freez.
Welti et al. (2018)	Atlantic	$\mathrm{INP\,m^{-3}}$	Airborne	CFDC, filter & drop freez.
Creamean et al. (2019)	Arctic	$\mathrm{INP\,L^{-1}}$	Airborne	Filter & drop freez.
Gong et al. (2019)	Cyprus	$\mathrm{INP\,L^{-1}}$	Airborne	Filter & drop freez.
Irish et al. (2019a)	Arctic	$\mathrm{INP\,L^{-1}}$	Airborne	Filter & drop freez.
Ladino et al. (2019)	Gulf of Mexico	$\mathrm{INP\,L^{-1}}$	Airborne	Filter & drop freez.
Si et al. (2019)	Arctic	$\mathrm{INP\,L^{-1}}$	Airborne	Filter & drop freez.
Wex et al. (2019)	Arctic	$\mathrm{INP\,L^{-1}}$	Airborne	Filter & drop freez.
Hartmann et al. (2020)	Arctic	$\mathrm{INP\,L^{-1}}$	Airborne	Filter & drop freez.
Gong et al. (2020)	Cabo Verde (Atlantic)	$\mathrm{INP\,L^{-1}}$	Airborne	Filter & drop freez.
Welti et al. (2020)	Arctic, Atlantic, Pacific, SO	$\mathrm{INP\,m^{-3}}$	Airborne	CFDC, filter & drop freez.

Table 1. Continued.

(ii) Studies investigating the ice-nucleating potential of seawater and SML samples				
Study	Loc.	Data	Subst.	Instr.
Birstein and Anderson (1953)	Artificial	Freez. T	Sea salt	Cloud chamber
Brier and Kline (1959)	Washington DC	INP L^{-1}	Seawater	Cloud chamber[1]
Schnell and Vali (1975)	Pacific (N/S), Caribbean, Atlantic	INP m^{-3}	Seawater	Drop freez.
Schnell and Vali (1976)	Canada, California, Bahamas	INP m^{-3}	Seawater	Drop freez.
Schnell (1977)	Atlantic (Canada)	INP m^{-3}	Seawater	Drop freez.
Parker et al. (1985)	Antarctica	FF	Sea ice	Drop freez.
Rosinski et al. (1988)	Gulf of Mexico	INP m^{-3}	Seawater	Cloud chamber[7]
Wilson et al. (2015)	Arctic, Canada, N. Pacific, Atlantic	FF, n_m	Seawater	Drop freez.
Irish et al. (2017)	Arctic	FF	Seawater	Drop freez.
McCluskey et al. (2017)	Lab (MART)	INP L^{-1}	Seawater	CFDC, filter & drop freez.
Irish et al. (2019b)	Arctic	INP L^{-1}, FF	Seawater	Drop freez.
Creamean et al. (2019)	Arctic	INP L^{-1}	Seawater	Drop freez.
Wilbourn et al. (2020)	North Atlantic	Freez. T, FF	Aerosolized seawater	Drop freez.
Gong et al. (2020)	Cabo Verde (Atlantic)	INP L^{-1}	Seawater	Drop freez.
Wolf et al. (2020)	Florida Straits, North Pacific	Active-site density	Seawater	CFDC
(iii) Studies concerned with the ice-nucleating potential of different phytoplankton species and their exudates				
Study	Loc.	Data	Subst.	Instr.
Schnell (1975)	Lab	INP m^{-3}	Phytoplankton	Drop freez.
Parker et al. (1985)	Lab	FF	Mar. bacteria	Drop freez.
Fall and Schnell (1985)	Lab	T_{50}	Mar. bacteria	Drop freez.
Alpert et al. (2011b)	Lab	Freez. T	Aqu. NaCl, diatoms	Drop freez.
Alpert et al. (2011a)	Lab	Freez. T	Phytoplankton	Drop freez.
Knopf et al. (2011)	Lab	Freez. T	Mar. diatoms	Drop freez.
Ladino et al. (2016)	Lab	FF	Phytoplankton, mar. bacteria	CFDC
McCluskey et al. (2017)	Lab	INP L^{-1}	Phytoplankton	CFDC, filter & drop freez.
DeMott et al. (2018a)	Lab	T_{50}	Fatty acids	Drop freez.
Tesson and Šantl Temkiv (2018)	Lab	Freez. T	Micro-algae	Drop freez.
Wilbourn et al. (2020)	North Atlantic	Freez. T	Phytoplankton	Drop freez.

are presented in an associate study; see Christiansen et al. (2020).

2.1 Samples and sample treatment

Two types of samples were investigated in this study: algal cultures (*Skeletonema marinoi* and *Melosira arctica*) and SML samples. One diatom species (*Skeletonema marinoi*) was grown under different conditions. The SML samples were collected during three field expeditions in the Arctic region (ACCACIA, Wilson et al., 2015; NETCARE, Irish et al., 2019b; and ASCOS, Gao et al., 2012). Table 2 provides an overview of how the samples were analysed and summarizes all the measurements conducted during this campaign.

2.1.1 Culture conditions and nutrient regimes for algae

The two diatoms were cultured axenically in Guillard's f/2+Si medium in 2 L glass bottles on a shaking table (0.5 rpm) inside a climate chamber. Algal growth rate and number of cells per colony were monitored using the cell counter TC20 (Bio-Rad). *Skeletonema marinoi* (CCAP 1077/5; Gothenburg University Marine Algal Culture Collection, GUMACC) was isolated from the Long Island Sound (Milford Harbor, USA). *Melosira arctica* (MATV-1402; Helsinki University) originated from the western Gulf of Finland, Baltic Sea.

Skeletonema marinoi (SM) was grown at 26 PSU (practical salinity unit) and 293.15 K using a 12 h : 12 h light–dark cycle at 90 µmol photons m^{-2} s^{-1}. Concentrations of nitrate and phosphate in the media were adjusted to conform to three experimental conditions in order to manipulate growth rates and cell carbon contents: (1) nutrient-replete conditions (SM100; high growth, high nutrient content of cells), (2) 60 % nutrient saturation (SM60; high growth but low nutrient content), and (3) low nutrient treatment (SM10; low growth, low nutrient content). The respective nitrate and phosphate concentrations were 5 and 1 µM in SM100, 3 and 0.6 µM in SM60, and 0.2 and 0.1 µM in SM10 treatments. Nutrients, but also their stoichiometric ratios, determine growth. In treatment (1), we had algae that were both dividing fast and had a large cell size. In treatment (2), the cell division rate was high, but the cell size was small (phosphorus limitation). In treatment (3), both parameters were low (nitrogen and phosphorus limitation). The algae were harvested (i.e. the entire culture volume was transferred to a plastic bag and frozen) when reaching a density of $\sim 3 \times 10^5$ and $\sim 5 \times 10^6$ cells mL^{-1} in the nutrient-replete and nutrient-sufficient (SM100 and SM60) conditions, respectively. Due to poor growth in SM10, the culture was harvested simultaneously with the other two treatments before reaching comparable cell densities.

Melosira arctica (MA) was grown at 6 PSU, 278.15 K, and a 16 h : 8 h light–dark cycle at 60 µmol photons m^{-2} s^{-1} and harvested when the concentration reached $\sim 2 \times 10^5$ cells mL^{-1}. This culture is referred to as MA100.

Immediately after collection, the harvested algae were frozen for storage and transport at 193.15 K. We assume that freezing the samples does not influence the results of the experiments, which is an assumption supported by the literature (Schnell and Vali, 1976; Irish et al., 2019b). Prior to freezing, a subsample of known volume from each species or treatment was collected on a 0.2 µm filter for dry weight (DW), C, and N analyses. The non-purgeable organic carbon content and the water activity of each sample were measured after the experiments. These values are summarized in Table 3.

2.1.2 Field samples

The SML samples were collected from different locations in the Arctic. A subset of the samples was collected during the Aerosol-Cloud Coupling and Climate Interactions in the Arctic (ACCACIA) expedition in July and August, 2013, in the Arctic Atlantic (east of Greenland and north of Spitsbergen; for more details see Wilson et al., 2015). Another subset of samples was collected as part of the Network on Climate and Aerosols: Addressing Key Uncertainties in Remote Canadian Environments (NETCARE) project during July and August 2016 in the eastern Canadian Arctic (for more details see Irish et al., 2019b). During ACCACIA and NETCARE, a remote-controlled sampling catamaran was used for collection (ACCACIA: Knulst et al., 2003; Matrai et al., 2008; NETCARE: Shinki et al., 2012). Previous analysis of these samples in terms of ice-nucleating ability can be found in the respective publications (Wilson et al., 2015; Irish et al., 2019b). The third subset of samples originates from the Arctic Summer Cloud Ocean Study (ASCOS) in August 2008 (Tjernström et al., 2014). The surface microlayer water was collected from an open lead using the same sampling catamaran used during the ACCACIA campaign. The sample investigated in this study was collected on 17 August 2008 at ca. 88° N and treated afterwards in three different ways. Two subsamples were subjected to a two-step ultrafiltration procedure. Firstly, the sample was passed through Millipore membrane filters (nominal pore size of 0.22 µm) under mild vacuum. Secondly, the filtered samples were ultra-filtered and diafiltered through a tangential flow filtration system (TFF, Millipore) equipped with cartridges with a molecular weight cutoff of 5 kDa. The fraction that passed through the 0.22 µm filters but not the TFF system is referred to as high-molecular-weight dissolved organic matter (5 kDa to 0.22 µm). To obtain even greater separation into low-molecular-weight dissolved organic matter, the sample which passed through the TFF system was further filtered in an Amicon® stirred cell (< 5 kDa). The third subsample is a foam layer sample. Seawater without pre-filtration was fed directly into a pre-cleaned glass tower (15.3 L, 2 m in height). Purified zero air was forced into the system through a sintered glass frit (nominal pore size of 15–25 µm) from the

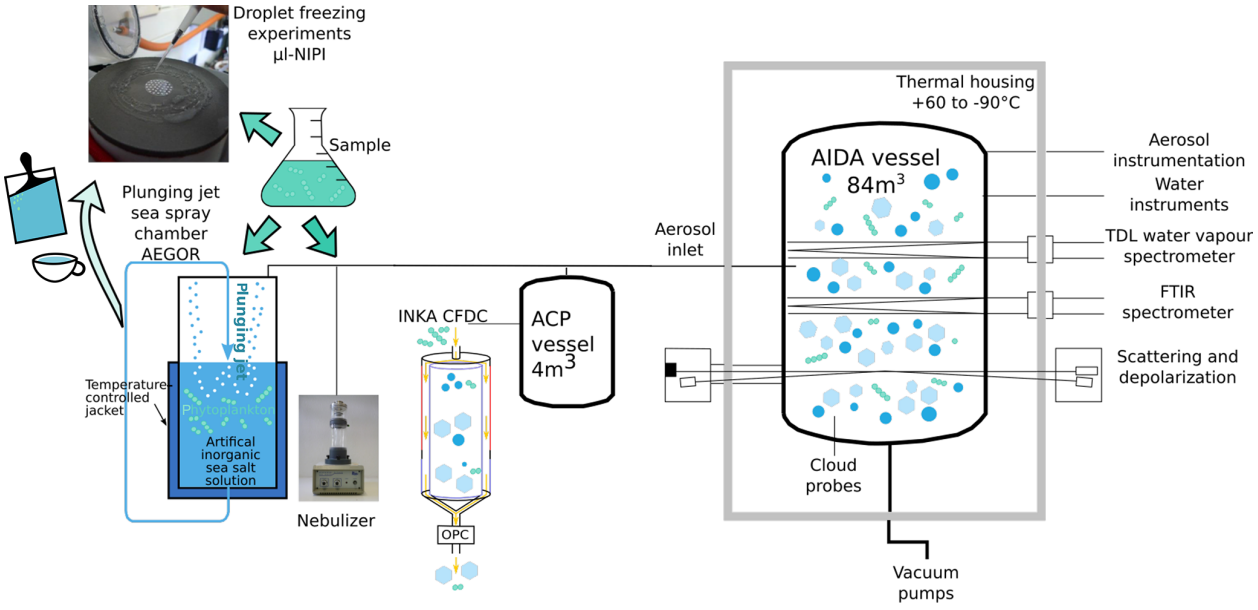

Figure 1. Schematic of the various aerosolization (AEGOR sea spray chamber and nebulizer) and ice nucleation (Aerosol Interaction and Dynamics in the Atmosphere (AIDA) aerosol and cloud chamber, Ice Nucleation Instrument of the KArlsruhe Institute of Technology (INKA), and microlitre nucleation by immersed particle instrument (µl-NIPI)) measurement techniques employed in this study.

bottom of the tower at a flow rate of 150 mL min^{-1}. After the bubble experiment, seawater at the uppermost layer (about 3 cm) together with foamy substances was slowly overflowed into a collecting flask by an additional feeding of seawater from the middle of the tower. The collected water from the top layer consisting of both foam and background seawater is referred to as the foam layer sample. The foam sample should be similar to an unfiltered SML sample (as obtained during ACCACIA and NETCARE). More details on the methods of filtration applied during ASCOS can be found in Gao et al. (2012).

All samples were immediately frozen at 193.15 K for storage and transport. The field samples are labelled according to the original names in the respective publications: the samples originating from the field expedition ACCACIA are called SML (purple, green, and turquoise colours in the figures), the samples from NETCARE are called STN (blue colours in the figures), and the samples from ASCOS are called ASCOS (red and yellow colours in the figures). The numbers refer to the original sample numbers.

2.2 Aerosolization techniques

Two different techniques were used to aerosolize samples for the AIDA cloud chamber. Firstly, undiluted samples were aerosolized using an ultrasonic nebulizer (GA2400, SinapTec) and injected directly into the AIDA chamber. An injection period of 20–30 min was sufficient to fill the AIDA chamber with an aerosol number concentration of approx. 550 cm^{-3}. Secondly, we used the temperature-controlled sea spray simulation chamber, AEGOR, with the aim of generating bubble-bursting aerosols in a more representative manner (Christiansen et al., 2019). The sea spray tank was filled with 20 L of artificial seawater (3.5 wt % solution of the synthetic Sigma-Aldrich sea salt mixture, product number S9883, in ultrapure water). Sigma-Aldrich sea salt is nominally purely inorganic and should not contain any biological or other ice-nucleating components. Thereafter, a certain volume of the investigated sample, as specified in Table 3, was added, and the aerosol generation process was started. The cell concentrations of algae in the AEGOR tank (see Table 3), ranging from 1 to 10^6 cells mL^{-1}, are representative for a strong phytoplankton bloom (Henderson et al., 2008; Borkman and Smayda, 2009; Saravanan and Godhe, 2010; Suikkanen et al., 2011; Canesi and Rynearson, 2016). In AEGOR, sea spray aerosols are generated by a plunging jet that entrains air into the sea spray tank and thus leads to bubble bursting, emitting aerosol particles to the headspace (flow rate of the jet was 5 L min^{-1}, nozzle diameter was 4 mm). Bubble formation using this technique mimics bubble formation through wave breaking. Bubbles rising through the water column scavenge surface-active organic material and transport it to the surface where it forms a microlayer. Subsequently, bubble bursting transfers this surface-active organic material to the aerosol phase.

Since the efficiency of particle generation by the sea spray simulation chamber was much lower than the nebulizer, injection of particles generated using this approach into the AIDA chamber was conducted over a period of 14–16 h, resulting in an aerosol particle concentration of approx. 300–400 cm^{-3}. Because of this time-consuming procedure, only

Table 2. Overview of the measurements conducted in this study. The first column lists all the different samples investigated (see Sect. 2.1), including information on the campaigns during which the field samples were collected. The type of sample is given in the second column. The aerosolization technique used for the AIDA measurements is denoted in the third column while the fourth column lists all the ice nucleation instruments used to probe the sample. The fourth column shows the date of the experiments. The fifth and six columns present the results of the fitted aerosol size distribution: the median particle diameter D and the width (geometric standard deviation) for all AIDA expansions (rounded to two digits).

Sample name	Type	Aerosolization techniques (AIDA)	Instruments	Date (AIDA expansion)	Fitted med. D (µm) (AIDA)	Fitted SD (AIDA)
Sigma-Aldrich sea salt	Artificial	Nebulizer, AEGOR	AIDA, µl-NIPI	27 Jan 2017, 30 Jan 2017, 6 Feb 2017	0.59 0.31 0.43	1.41 2.34 2.68
SM100	Cultured	Nebulizer, AEGOR	AIDA, µl-NIPI, INKA	6 Feb 2017, 21 Feb 2017, 7 Feb 2017, 8 Feb 2017	0.71 0.76 0.43 0.46	1.38 1.37 2.46 2.23
SM60	Cultured	Nebulizer	AIDA, µl-NIPI, INKA	8 Feb 2017	0.73	1.43
SM10	Cultured	Nebulizer, AEGOR	AIDA, µl-NIPI, INKA	16 Feb 2017, 17 Feb 2017	0.72 0.49	1.47 2.83
MA100	Cultured	Nebulizer, AEGOR	AIDA, µl-NIPI, INKA	22 Feb 2017, 23 Feb 2017	0.41 0.74	1.33 2.8
STN2 (NETCARE)	SML	Nebulizer	AIDA, µl-NIPI	10 Feb 2017	0.82	1.30
STN3 (NETCARE)	SML	Nebulizer	AIDA, µl-NIPI, INKA	15 Feb 2017	0.77	1.38
STN7 (NETCARE)	SML	Nebulizer	AIDA, µl-NIPI, INKA	15 Feb 2017	0.77	1.39
SML5 (ACCACIA)	SML	Nebulizer, AEGOR	AIDA, µl-NIPI, INKA	1 Feb 2017, 2 Feb 2017	0.59 0.7	1.47 2.61
SML8 (ACCACIA)	SML	Nebulizer, AEGOR	AIDA, µl-NIPI, INKA	31 Jan 2017	0.88 0.40	1.21 2.9
SML16 (ACCACIA)	SML	Nebulizer	AIDA, µl-NIPI, INKA	3 Feb 2017	0.86	1.25
SML17 (ACCACIA)	SML	Nebulizer	AIDA, µl-NIPI, INKA	9 Feb 2017	0.83	1.36
SML19 (ACCACIA)	SML	Nebulizer	AIDA, µl-NIPI, INKA	3 Feb 2017	0.90	1.27
ASCOS (< 5 kDa)	SML	Nebulizer	AIDA, µl-NIPI	23 Feb 2017	0.75	1.43
ASCOS (foam)	SML	Nebulizer	AIDA, µl-NIPI	24 Feb 2017	0.85	1.3
ASCOS (5 kDa to 0.22 µm)	SML	Nebulizer	AIDA, µl-NIPI	24 Feb 2017	0.18	1.27

a subset of the bulk solutions was used for aerosol generation with AEGOR (Table 2). The temperature of the AEGOR tank was set to 293.15 K for the SM culture samples, 277.15 K for the MA culture sample, and 275.15 K for the SML samples.

Aerosolizing an SML sample with a nebulizer is very different from aerosolization due to bubble bursting for a number of reasons. Firstly, only a small volume of sample is required for nebulization, so pure SML samples could be aerosolized (we had limited sample volume); the sea spray simulation chamber requires a higher volume of sample, so samples were added to 20 L of artificial seawater (we used up to 900 mL sample volume). As such, the SML samples underwent significant dilution when added to artificial seawater in the sea spray simulation chamber. Secondly, the process of aerosol generation by bubble bursting is quite different to aerosol generation in a nebulizer. As such, those aerosols generated in the sea spray simulation chamber are likely more representative of aerosols generated by oceanic bubble bursting (Collins et al., 2014; King et al., 2012; Prather et al., 2013). Given these differences, comparison of the ice activity of aerosol generated by these two techniques should enable us to determine whether INP material is preferentially aerosolized by bubble bursting.

Table 3. Characteristics of the bulk samples used during the study: non-purgeable organic carbon content; water activity of the artificial seawater, algal cultures, and two SML samples; the algal cells per mL of the cultures; and the carbon cell contents of the cultures. For the diluted samples, we give in parentheses how many millilitres of sample was added to 20 L of artificial seawater (3.5 wt % solution of the synthetic Sigma-Aldrich sea salt mixture in ultrapure water) in the AEGOR sea spray tank (see Sect. 2.2). For the samples indicated with "pure", the undiluted sample was used. The water activity of the samples was estimated directly using the dew point. These measurements were repeated three times, resulting in the standard deviation (SD) values given here.

Sample name	Non-purgeable organic carbon ($mgC\,L^{-1}$)	Water activity (dew point)	Water activity SD (dew point)	Algae cells (mL^{-1})	Carbon cell content ($\mu gC\,mL^{-1}$)
SM100 (pure)	14.3	0.9871	0.0004	5 280 000	105.6
SM10 (pure)	5.1	0.9916	0.0005	350 000	9.8
MA100 (pure)	10.9	0.9861	0.0006	188 700	245.31
Sigma-Aldrich sea salt (pure)	1.1	0.9854	0.0004		
SM100 (79 mL in AEGOR)	2.3	0.9861	0.0008	20 774	0.42
SM100 (406 mL in AEGOR)	1.7	0.9838	0.0006	105 051	2.1
SM10 (approx. 900 mL in AEGOR)	0.9	0.9855	0.0002	15 072	0.42
MA100 (893 mL in AEGOR)	3.2	0.9861	0.0006	1	10.49
SML8 (200 mL in AEGOR)	1.6	0.9866	0.0004		
SML5 (100 mL in AEGOR)	1.1	0.9857	0.0002		

We expect that aerosolization of the samples with the nebulizer results in an upper estimate of INPs; this is because the undiluted SML (or cultured) samples are aerosolized, whereas AEGOR is aerosolizing a dilution of the samples with artificial seawater, which could result in a lower estimate of INPs. However, it is not just the dilution factor in the sea spray simulation chamber (see Table 3) which has to be accounted for. The aerosolization process itself is different in AEGOR compared to the nebulizer. In the nebulizer, the suspension is well mixed, while in AEGOR the aerosol particles are formed from an organic-enriched surface microlayer at the top of the tank. That leads to different expectations depending on the sample type. For the SML samples, we would not expect such a huge difference due to this aspect. Here, we aerosolize in one case the pure well-mixed SML (nebulizer), while in the other case we aerosolize the SML that has formed in AEGOR, which should be similar to the original SML sample. For the cultured samples, however, we would expect a larger influence. In AEGOR the phytoplankton material is floating at the surface of the tank, leading to organic-enriched aerosol particles during the aerosolization, while the nebulizer might produce less enriched aerosol particles due to the mixing of the sample. Note that this might depend on the algal culture as well. Another crucial aspect of the two different aerosolization methods is the size distribution and the resulting chemical composition of the generated aerosol. It was demonstrated in the laboratory and as well measured in the field that for sea spray aerosol the organic composition of the aerosol particles and the generated size distribution are related (O'Dowd et al., 2004; Prather et al., 2013). One interesting aspect of our study is to see the influence of all the aspects mentioned above and to check if the diluted samples aerosolized with AEGOR show a similar or a lower freezing signal compared to the aerosolized pure samples.

2.3 Aerosol size and number measurements

The aerosol particle number concentration was measured using a condensation particle counter (CPC3010, TSI). The aerosol particle number size distributions were measured with a scanning mobility particle sizer (SMPS, TSI; mobility diameter of 0.014–0.820 µm) and an aerodynamic particle spectrometer (APS, TSI; aerodynamic diameter of 0.523–19.81 µm). In the AIDA chamber, typically held at 250 K and a relative humidity of 78 % during aerosol injection (see Sect. 2.4 for more details and an explanation of the low temperature), the aerosol particles were suspended as supercooled aqueous solution droplets. It is important to consider, however, that the size distribution measurements were done at room temperature (298 K) by sampling air from the cold interior of the aerosol chamber (Fig. 1). The water vapour content at 250 K corresponds to a relative humidity of only 2.4 % after warming to 298 K (Murphy and Koop, 2005). We thus assume that the measured size distributions represent the effloresced, dry particle sizes of the algal culture and SML particles (Koop et al., 2000). A dynamic shape factor of 1.08 and a particle density of $2.017\,g\,cm^{-3}$ (Zieger et al., 2017) for sea salt were used to convert the mobility and aerodynamic diameters of the SMPS and APS measurements into the volume-equivalent spherical diameters. Figure 2 shows the combined size spectra of the SMPS and APS measurements, which is plotted as surface area size distributions, for

two exemplary aerosol particle populations produced by the nebulizer and AEGOR (SM100 and SML8).

The comparison of both aerosolization techniques for the algae and the field samples shows that the nebulizer produces rather uniformly sized particles with a median diameter of about 0.8 µm in the surface area size distributions. In contrast, the bubble-bursting process simulated in AEGOR leads to a much broader surface area size distribution with a smaller median diameter. However, both the nebulizer and AEGOR are not producing very narrow size distributions (see Fig. 2). The majority of our aerosolized samples yielded surface area size distributions that are very similar to those shown in Fig. 2. For each sample, a log-normal fit was created based on least squares. The fits are expressed as a function of the median equal-volume sphere diameter, the geometric standard deviation, σ, and the aerosol surface area concentration. The median diameter of the particles generated with the nebulizer was typically in the range from 0.71 to 0.90 µm with a distribution width, σ, between 1.21 and 1.47. Smaller particles with median diameters of 0.59, 0.41, and 0.18 µm were obtained for the SML5, MA100, and ASCOS high-molecular-weight (high molec. weight, 5 kDa–0.22 µm) samples, respectively, which is probably related to lower salt concentrations in the respective solutions. Aerosol generation with AEGOR yielded median diameters between 0.4 and 0.7 µm and distribution widths, σ, between 2.2 and 2.9.

2.4 Ice nucleation measurement techniques

The combination of instrumental methods used in this study facilitates measurement of the ice-nucleating ability of marine organic aerosols over a wide temperature range. The ice nucleation activity was measured using three different ice nucleation instruments: AIDA, INKA, and the µl-NIPI, which all have their highest sensitivities in different temperature ranges. While the µl-NIPI is sensitive in the temperature regime above 248 K, AIDA and INKA are only sensitive in the temperature regime below 248 K for the type of samples analysed in this study. All three measurement techniques are explained in detail in the following sections.

AIDA

The AIDA facility comprises two aerosol chambers (Fig. 1) (Möhler et al., 2008). The term AIDA chamber refers to the 84.3 m^3 sized aluminium vessel that is enclosed in an isolating containment and can be operated at any temperature between ambient and 183 K. A smaller 3.7 m^3 sized stainless-steel vessel is located in the vicinity of AIDA. It is referred to as the APC (aerosol preparation and characterization) chamber and can only be operated at ambient temperature. As indicated in Sect. 2.2, the aerosol particles were directly injected into the AIDA chamber to probe their ice nucleation activity by expansion-cooling experiments. For practical reasons, the same aerosol particles were additionally injected into the APC chamber, acting as a reservoir for long-term measurements of the particle ice nucleation behaviour with the INKA instrument (see next section) and for the CCN measurements (see Christiansen et al., 2020).

The operation of the AIDA chamber as a cloud simulation chamber for studying ice nucleation has been thoroughly described previously (Möhler et al., 2003, 2005; Wagner and Möhler, 2013). Briefly, a mechanical pump is used for a controlled reduction of the chamber pressure starting from ambient to about 800 hPa. Expansion cooling generates supersaturations with respect to ice and/or supercooled liquid water, triggering the formation of ice crystals and supercooled water droplets by various nucleation mechanisms (Vali, 1985; Vali et al., 2015). In the present study, the ice nucleation activity of the algal cultures and SML samples was investigated in the immersion freezing mode at mixed-phase cloud temperatures. For aerosol injection, the AIDA chamber was typically held at a temperature of 250 K and a relative humidity with respect to supercooled water (RH_w) of about 78 %, as controlled by an ice layer on the inner walls of the aluminium vessel. RH_w was measured in situ by tuneable diode laser (TDL) absorption spectroscopy with an uncertainty of ±5 % (Fahey et al., 2014). With increasing RH_w during expansion cooling, the injected aqueous solution droplets continuously took up water vapour from the gas phase, and they were finally activated to ≥ 10 µm sized cloud droplets when RH_w exceeded 100 %. The number concentration and size of the cloud droplets were measured with two optical particle counters (OPCs) welas® 1 and 2 (Palas GmbH) with an overall detection range of 0.7–240 µm. Cloud formation was typically observed after 3 K of expansion cooling, i.e., at a temperature of about 247 K. Whereas pure supercooled water droplets would only freeze homogeneously when the gas temperature further dropped to about 238 K during expansion cooling (Benz et al., 2005), the activated algal culture and SML aerosol particles exhibited heterogeneous ice nucleation modes due to immersion freezing at temperatures above 238 K. The number concentration of the nucleated ice crystals, N_{ice}, was separately deduced from the OPC records by using an optical threshold size to subtract the scattering signals of the smaller-sized supercooled cloud droplets. By dividing N_{ice} through the seed aerosol particle number concentration, the ice-active fraction, FF, of the aerosol particle population was calculated. By further dividing FF through the average dry surface area of a particle, A_{aer} (determined from the size distribution measurements shown in Fig. 2), the ice nucleation active-surface-site density, n_s, of the polydisperse particle population could be computed (e.g. Hoose and Möhler, 2012):

$$n_s(T) = \frac{\mathrm{FF}(T)}{A_{aer}}. \quad (1)$$

This equation is an approximation, which is valid for small values of FF(T) (Hoose and Möhler, 2012) and was tested

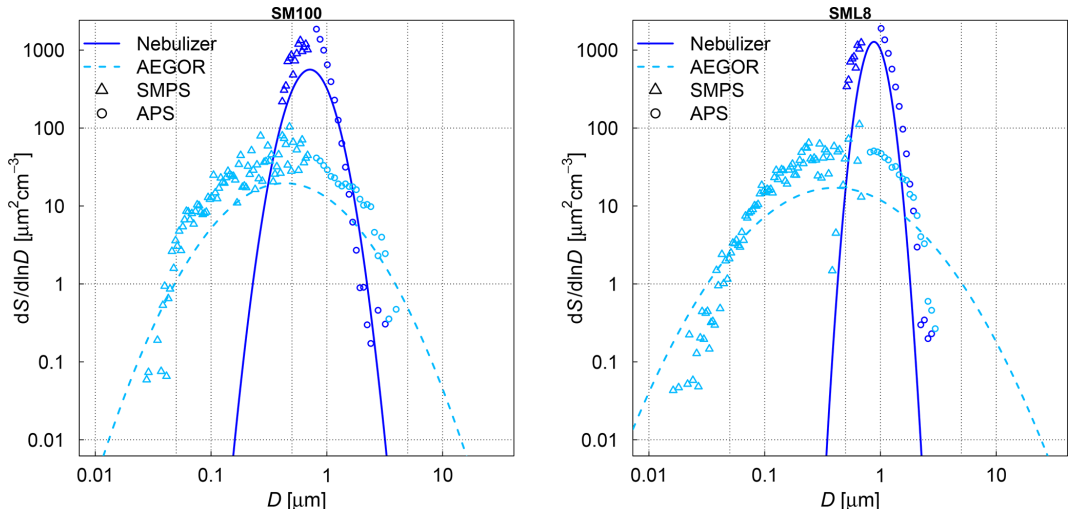

Figure 2. Measured size distributions and fits to the data for two different samples: an algal sample (SM100) and a field sample (SML8). The samples were aerosolized using a nebulizer (solid line) or the AEGOR sea spray simulation chamber (dashed line). The aerosol size measurements are done with an APS (circles) and a SMPS (triangles). D denotes the equal-volume sphere diameter of the aerosol particles, and S is the surface area concentration.

to be applicable for the dataset presented here. It is also assumed that n_s is independent of size.

The uncertainty of the deduced ice nucleation active-surface-site densities (n_s) was estimated to be ±40 % (Ullrich et al., 2017).

In the following we estimate a lower detection limit of n_s in the AIDA experiments. The minimum detectable ice particle number concentration, as limited by the size of the detection volume of the OPC sensors, is about 0.05 cm^{-3}, equalling to one detected ice crystal in a sampling period of about 10 s. Together with the typical seed aerosol particle number concentration of about 500 cm^{-3} (Sect. 2.2), the lower detection limit for FF can thus be estimated to be about 10^{-4}. The average dry surface area of the aerosol particles generated with the nebulizer was around 1 μm^2, yielding a lower detection limit for n_s of about 10^8 m^{-2} (Eq. 1). In comparison to recent literature n_s values for laboratory and field sea spray aerosol particles (DeMott et al., 2016), n_s only exceeded such values at temperatures below about 248 K. This illustrates why the starting temperature of the expansion-cooling runs was chosen as low as 250 K, limiting the ice nucleation data to temperatures below about 247 K. During our study, we also probed a number of samples (STN2, STN3, and SM100) at a higher starting temperature of 258 K. However, we did not observe any ice formation above the detection limit down to a temperature of 248 K. For this reason, the AIDA data cover the above-defined low-temperature regime of the ice nucleation spectra.

In addition to the expansion-cooling cycles with the algal and SML samples, we conducted three control runs with the synthetic Sigma-Aldrich sea salt mixture, using both AEGOR and the nebulizer for aerosol generation. Here, the deduced n_s values were close to the estimated detection limit of 1×10^8 m^{-2} at temperatures between 247 and 238 K. The small concentration of heterogeneously formed ice crystals could be due to traces of insoluble components in the synthetic salt mixture or due to ice nucleation on background aerosol particles in the cloud chamber. All aerosols exhibited n_s values 2–50 times larger than this background signal (see Sect. 3.2). To account for possible contamination originating in the nebulizer or AEGOR, a background subtraction was conducted using these reference experiments with a pure Sigma-Aldrich sea salt solution and subsequent estimation of the average background n_s value. The estimated background from these reference experiments was consistent and independent of temperature; it was higher for AEGOR compared to the nebulizer, probably due to the more complex setup of aerosolization in the former.

INKA

Most of the samples that were probed in the AIDA chamber were also tested for their ice nucleation activity using the INKA cylindrical continuous-flow diffusion chamber (Schiebel, 2017). As explained above, the APC chamber was used as an aerosol particle reservoir for the INKA measurements. The APC chamber was held at 298 K and RH < 5 %, meaning that the injected solution droplets generated with the nebulizer or AEGOR readily effloresced to form crystalline particles. Upon injection into the INKA instrument, aerosols are exposed to well-controlled temperature and relative humidity conditions by flowing through a chamber with iced walls held at different temperatures. The sample air flow is sheathed by particle-free synthetic air (initially dry) in order to position the aerosol lamina between the walls and to

allow for the calculation of the thermodynamic conditions within the lamina (Rogers, 1988). The residence time of the aerosol is 10 to 15 s, depending on the actual settings. Any droplets that might have formed in this section will shrink in a subsequent chamber section with no temperature difference between the iced walls. The formed ice particles will persist in this so-called evaporation section. The thus increased size difference between droplets and ice particles at the chamber outlet allows for an easy ice particle detection with an optical particle counter (Climet CI-3100). INKA scans the ice nucleation activity by continuously increasing the sample's relative humidity at constant temperature settings. Due to a larger detection volume of the Climet OPC compared to the welas® sensors used in the AIDA experiments, the lower detection limit for n_s with INKA is about $10^7\,\mathrm{m}^{-2}$. In intercomparison studies using natural soil dust aerosol (DeMott et al., 2018a) or commercially available cellulose particles (Hiranuma et al., 2019), INKA has shown a good agreement with AIDA and other ice nucleation instruments. In the present study, most experiments have been conducted above 241.15 K to enable a clear differentiation from homogeneous freezing events and to allow for direct comparison with AIDA results.

µl-NIPI

The µl-NIPI is a cold-stage instrument, which is used with a substrate to probe the ice nucleation in immersion mode of microlitre (µL) volume droplets (Whale et al., 2015). To do so, the droplets of the sample under investigation (if not explicitly otherwise mentioned, this is a bulk sample) are pipetted onto a silanized glass slide, which serves as a hydrophobic substrate. It is a "bulk" technique analysing the suspension directly under the assumption that the sample is well mixed so that particles are distributed randomly, and each droplet is representative of the sample as a whole, meaning each one has an approximately equal probability of containing an INP that is active at a given temperature. The droplets are then cooled at a rate of $1\,\mathrm{K\,min}^{-1}$ until the droplets are all frozen. The temperature values of the individual freezing events are optically detected using a camera and offline analysis. The number of droplet-freezing events detected throughout the temperature ramp are then converted into a fraction frozen at each temperature. This fraction frozen, or FF curve, represents the raw freezing events. In order to calculate a concentration of INP per liquid unit volume of sample, $K(T)$, the FF must be thought of as the probability of freezing, and so the equation below can be used to deduce the cumulative nucleus concentration per unit volume of sample used (Vali, 1971):

$$\mathrm{FF}(T) = \frac{N_{\text{frozen droplets}}(T)}{N_{\text{droplets}}}, \tag{2}$$

$$K(T) = \frac{-\ln(1-\mathrm{FF}(T))}{V_{\text{droplet}}} \cdot D\ , \tag{3}$$

where V_{droplet} is the volume of a droplet, N_{droplets} is the total number of droplets on the cold stage at the beginning of the freezing experiment, $N_{\text{frozen droplets}}$ is the number of droplets frozen at a certain temperature, and D is the dilution factor relative to the undiluted sample, which is relevant for the samples coming from AEGOR and a couple of dilution experiments conducted with the algal cultures (in all other cases D is 1).

$K(T)$ can then be weighted to physical aspects of the sample such as the surface area of the particles or the mass of salt in the sample in order to directly compare to other instruments using the same sample.

In contrast to AIDA and INKA, the µl-NIPI is sensitive to INP in a relatively high temperature range. Given the relatively large size of the pipetted droplets, this technique is better suited to the investigation of freezing by rare INPs; i.e. there is a greater probability of having an INP within the droplet which subsequently freezes the whole droplet.

3 Results

In this section, we first address the ice nucleation measurements with the µl-NIPI instrument in the temperature regime above 248 K (Sect. 3.1). The AIDA and INKA results for temperatures below 248 K are presented in Sect. 3.2. Finally, Sect. 3.3 outlines an approach to combine the AIDA/INKA and µl-NIPI data into a single dataset to examine the ice nucleation behaviour of the algal cultures and Arctic SML samples over the full temperature range relevant for freezing in the mixed-phase cloud regime.

3.1 Temperature regime above 248 K (bulk samples)

The frozen-fraction curves measured with µl-NIPI for the field and algal samples are shown in Fig. 3. Among the field samples, there is a large spread in ice nucleation activity with a median freezing temperature T_{50} (FF = 0.5, i.e. half of the droplets are frozen) of approx. 262 to 245 K (i.e. a spread of 17 K). While the ice nucleation is very variable throughout the samples, the dependence on temperature (slope of the curves) is mostly similar. A number of the samples exhibited ice nucleation activity at relatively high temperatures (> 263.15 K), with the ASCOS high-molecular-weight sample (ASCOS high molec. weight, 5 kDa to 0.22 µm) and SML5 being the most ice active. Both algal samples studied were also ice active, although they were clearly less ice active than the field samples despite their relatively high cell concentration (compared to natural seawater). For example, the T_{50} of the culture samples is approx. 252 to 246 K (range of 6 K), which is within the colder part of the variability of the field samples (see Fig. 3a). Furthermore, no large differences (a difference of T_{50} of approx. 5 K) were observed between the different diatom species or when comparing the different nutrient conditions for SM. However, it should be

noted that there was variability within the individual cultures and that storage changed the ice nucleation activity. For example, the same SM100 culture was delivered to AIDA in two separate bags. We refer to one bag as SM100a and the other one as SM100b. A third sample (SM100c, a subsample of SM100b) was analysed 2 months after the campaign after having been stored at or below 253 K. SM100d, also a subsample of SM100b, was used for some further tests 10 months after the campaign (as well stored at or below 253 K). Note that the results of SM100d should be used with caution and not directly compared to the other ones, since this sample was unfrozen several times and stored for quite a long period of time, which might not be ideal.

Comparing SM100a, SM100b, and SM100c, it can be seen that the freezing properties of the SM100 sample are variable. SM100a and SM100b look similar, with most of the spectrum at low temperature in the background. They show differences at higher temperatures, where SM100a displayed activity but SM100b did not. SM100c showed different activity from SM100a and SM100b with the freezing shifted to higher temperatures that leads to the whole curve being outside of the background (compared to SM100b). The gradients between all three curves are also different, with SM100a having the shallowest slope. Additional to the variability of the sample itself (different bags – SM100a and SM100b), it seems that the sample changed with time, so age, storage, and multiple freezing cycles may all have had effects on the sample.

The STN samples have been analysed previously using a similar droplet-freezing technique, albeit using a 10 times faster cooling rate ($10\,\mathrm{K\,min^{-1}}$) (Irish et al., 2019b). Comparison of these measurements with our measurements of the same samples highlight the differences. We observed up to an order of magnitude higher $K(T)$ values (and up to a 10 K difference for the same $K(T)$) than those reported in Irish et al. (2019b), which might have been influenced by the difference in the cooling rate. The temperature at which 50 % of the droplets are frozen has been shown to decrease with increased cooling rate in Wright and Petters (2013) and Herbert et al. (2014); also, this dependence was shown to be rather small. Nevertheless, a shift of 10 K for a factor of 10 change in cooling rate is unlikely. The SML samples from Wilson et al. (2015) were analysed using the same droplet-freezing technique as in this study. Samples SML5, SML8, and SML16 exhibited ice activity at similar temperatures to those presented in Wilson et al. (2015), while samples SML17 and SML19 exhibited lower ice activity, with lower temperatures of freezing for the same fraction frozen. Therefore, we conclude that some samples were unaffected by long-term storage (being frozen at 193.15 K), while the activities of other samples changed. This indicates that some ice-active components are altered through the freezing, storage, and thawing process. Note that this contradicts earlier assumptions based on findings of Schnell and Vali (1976) and Irish et al. (2019b). However, Polen et al. (2016) has shown that the biological INP Snomax® is sensitive to storage. An alteration of INP characteristics of our microlayer samples indicates that they contain different ice-active components which have different properties and may be related to different biological processes. In this paper we use the remeasured droplet-freezing results to compare the ice nucleation activity between instruments.

The influence of bubbling the samples in the AEGOR sea spray chamber on the ice nucleation activity was investigated by comparing pure samples with three different subsamples taken out of AEGOR after bubbling: one bulk subsample (collected from the bottom of AEGOR), one scoop subsample (collected by scooping a falcon tube along the surface liquid), and a microlayer subsample (collected by the glass-plate technique as per the methods of Harvey, 1966). Note that all these samples are bulk samples. Upon introduction to AEGOR, there was a significant dilution of the sample with artificial seawater (Table 3). The ice nucleation activity of the SML5 subsamples as described above is shown in Fig. 4. To take the dilution into account, the data are plotted with respect to the volume of sample used, as $\mathrm{INP\,L^{-1}}$ (see Eq. 3). Interestingly, the bulk and microlayer subsamples exhibit lower ice activity than the scoop subsample. However, it is important to note that most points from the bulk and microlayer samples are in the baseline of the µl-NIPI experiment, and can therefore be seen as upper limits. It is notable, however, that the "microlayer" sample obtained with a glass plate had a lower activity than scooping the surface water, which might suggest that the ice-active components may only have an intermediate affinity for the glass plate. Nevertheless, the fact that the upper layers of water in AEGOR are enhanced in INP suggests that organic INP material scavenged by bubbles resides at the water surface and is likely surface active (i.e. material which preferentially resides at an interface). As such, this material may be scavenged by the bubbling in the chamber and be preferentially aerosolized during the bubble-bursting process.

3.2 Temperature regime below 248 K (aerosolized samples)

The ice nucleation results of the AIDA and INKA measurements, expressed as ice nucleation active-site densities versus temperature $n_s(T)$, are shown in Fig. 5 (SML samples) and Fig. 6 (algal cultures). With respect to the experiments where AEGOR was used for aerosol generation, some samples did not exhibit a detectable freezing signal above the background (SM100, SM10, and SML8) and are therefore not included. As a comparison to our data, Fig. 5 includes a recently published dataset consisting of field measurements of sea spray aerosols and laboratory data of particles released during an algae bloom generated in a marine aerosol reference tank (DeMott et al., 2016). Furthermore, we show a parameterization of the temperature-dependent n_s values for desert dust particles (Niemand et al., 2012).

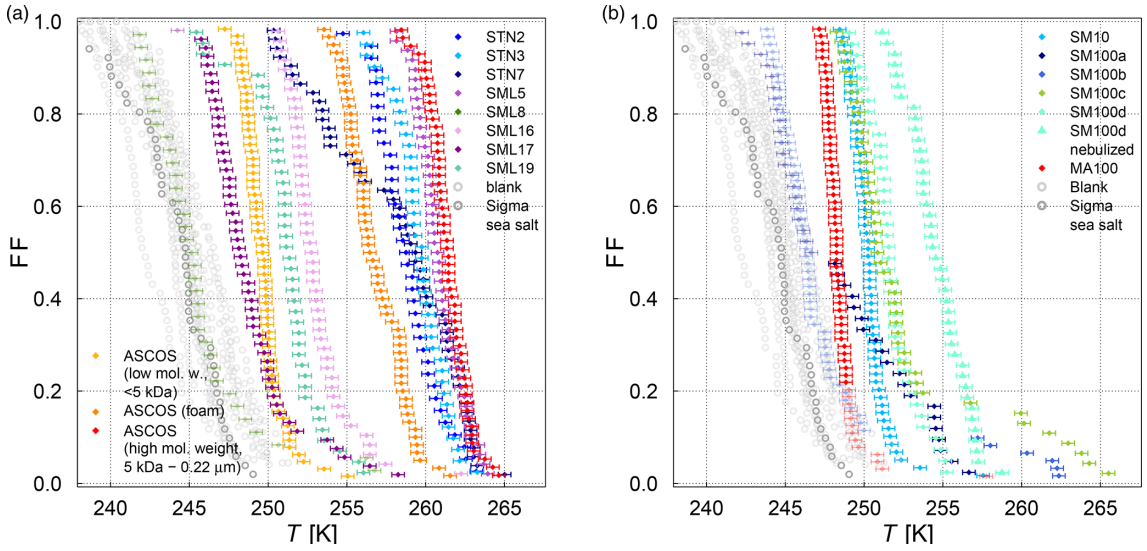

Figure 3. Fraction frozen curve (a measure of the fraction of droplets frozen at discrete temperatures) for **(a)** nine different SML field samples coming from three different Arctic field expeditions (ACCACIA, NETCARE, ASCOS) measured with the µl-NIPI (droplet-freezing technique, bulk, undiluted samples). The field sample from ASCOS was treated in three different ways (see Sect. 2.1.2). **(b)** Two cultured diatom species measured with the µl-NIPI (droplet-freezing technique, bulk): *Skeletonema marinoi* (SM) and *Melosira arctica* (MA). The SM sample was investigated for two different nutrient regimes (see Sect. 2.1.1). Two duplicate samples of SM100 (SM100a and SM100b) are reflecting the variability of the sample. SM100a and SM100b are from two bags collected from the same culture. SM100c is a subsample of SM100b after 2 months storage. SM100d, a subsample of SM100b, was in storage for 10 months, and it was then nebulized and retested to determine the effect of the aerosolization on the sample. The points with reduced opacity represent upper limits for those data points, as they could have been affected by background signal. Note that the temperature in both plots was not corrected for freezing-point depression caused by salts, because the water activity was not available for all samples.

The various SML samples show little variation at temperatures below 248 K when probed in the AIDA chamber, meaning that the SML samples all exhibited similar ice nucleation activity (n_s of $10^9\,m^{-2}$ at temperatures between 240 and 244 K) and the individual $n_s(T)$ curves of the AIDA measurements form a rather compact block of data (Fig. 5). One notable exception is the ASCOS high-molecular-weight sample (ASCOS high molec. weight, 5 kDa to 0.22 µm). Whereas the foam and < 5 kDa ASCOS samples fall into the range of n_s values observed for the other SML and STN microlayer samples, n_s for the high-molecular-weight sample is about 1 order of magnitude higher. This agrees with the µl-NIPI observations, where this particular sample also proved to be one of the most ice active. The ASCOS high-molecular-weight sample consists of the high-molecular-weight dissolved organic matter of the collected SML sample. More specifically, it was shown in Orellana et al. (2011) and Gao et al. (2012) that this sample mostly contained marine colloidal gels. This might lead to an enrichment of ice-active organic material and explains the high ice nucleation activity of this sample. Note that this sample is highly concentrated. The size range of the filtration of the sample indicates that macromolecules are responsible for the freezing of the sample. Most bacteria, cell debris, etc. are likely to be removed by the ultrafiltration. The size distribution of the nebulized ASCOS high-molecular-weight sample resulted in particles with the smallest diameters compared with other samples, which might have an influence on the ice nucleation activity as well since the chemical composition of sea spray aerosol is highly size dependent. This sample might consist of smaller particles with a larger organic mass fraction compared to the other samples. Other field samples that proved to be particularly ice active in the high-temperature regime like SML5, however, do not show superior ice nucleation activity at temperatures below 248 K. This is an indication that different types of ice-active material might cause freezing in the different temperature ranges, which is an issue that will be further discussed in Sect. 3.3 when combining the AIDA and µl-NIPI datasets.

In order to facilitate the comparison of the AIDA measurements with previous studies of ambient marine aerosols, we chose to represent the DeMott et al. (2016) data in Fig. 5 by a grey shaded area that encompasses the observed range of nucleation site density values n_s. A similar representation was used by McCluskey et al. (2017), who have determined n_s for nascent sea spray aerosol particles during phytoplankton blooms in the laboratory. These data are not separately depicted because they fall into the regime of the DeMott et al. (2016) dataset. A particular subset of the DeMott et al. (2016) data is highlighted in Fig. 5 by the grey stars. These data points refer to a laboratory experiment in the Marine Aerosol Reference Tank (MART) following the peak of the

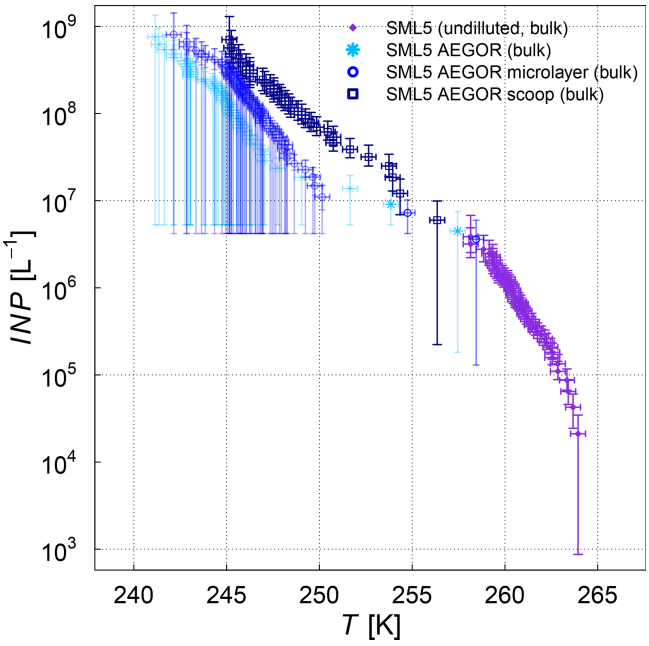

Figure 4. Cumulative INP concentration per unit volume of the SML5 field sample for the pure sample in comparison to different dilutions (subsamples from AEGOR: bulk, microlayer, scoop; see text for details). Where the lower error bar is unchanged from the previous point, there may have been no additional INP detected above the background signal. Note that the temperature in this plot was not corrected for freezing-point depression caused by salts because the water activity was not available for all samples.

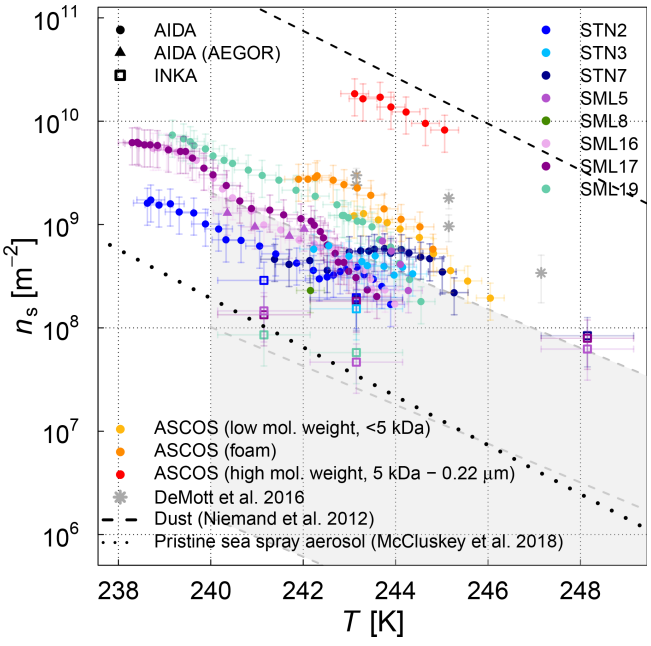

Figure 5. Surface-active-site density n_s as a measure for ice nucleation activity at different temperatures for 11 different SML samples from the AIDA (coloured full circles and triangles) and INKA (open squares) measurements. The field sample from ASCOS was treated in three different ways (see Sect. 2.1.2). Different symbols show the different aerosolization techniques for the AIDA measurement (nebulizer in circles, AEGOR in triangles). The AIDA n_s data were corrected for the background ice nucleation mode observed in the reference experiments with purely inorganic Sigma-Aldrich sea salt solution droplets (see Sect. 2.4). The data of DeMott et al. (2016) are shown as a grey shaded area (fit and shifted fits to the upper and lower limits of the data) and grey stars (MART phytoplankton bloom); see text for details.

phytoplankton bloom. The n_s values derived from the AIDA measurements for the field samples fall into the range of former observations, albeit towards the upper more-ice-active regime of the data by DeMott et al. (2016). The MART data for the artificially enhanced phytoplankton bloom are in good agreement with the upper thresholds of n_s for our field samples. Given that most of the AIDA measurements were made by aerosolizing the undiluted SML solutions with the nebulizer, it can be expected that this dataset indeed represents an upper limit of the ice nucleation activity of natural sea spray aerosol particles.

The experiments where AEGOR was used for aerosol generation shed some light on how much of the ice-active material in the SML bulk solutions may be released during the process of air entrainment, bubble scavenging, and bubble bursting. For both sample types investigated (the algal cultures and natural SML samples), we find examples where the ice nucleation activity observed for particles generated using the AEGOR tank remains similar to the ice activity of aerosols generated by nebulizing the pure sample despite the strong dilution of the samples with artificial seawater in the AEGOR tank (SML5, Fig. 5; MA100, Fig. 6). This suggests that, in some cases, the organic INP material is indeed preferentially scavenged by the bubbling in the seawater tank and aerosolized during the bubble-bursting process. For other samples, however, the ice nucleation activity was reduced to below the detection limit (n_s of 10^8 m^{-2}) after the dilution in AEGOR (SML8, SM10, and SM100). This variability in the AEGOR experiments might explain why the previous field measurements of sea spray aerosol particles show a huge spread in the n_s values, whereas the laboratory nebulizer data fall into a narrow range at the upper end of the ice nucleation activity scale. Note that this upper limit of the ice nucleation activity of the field samples, however, is still 1 order of magnitude lower than the n_s parameterization for mineral dust (Fig. 5, Niemand et al., 2012), underlining the relatively poor heterogeneous ice nucleation activity of sea spray aerosol particles compared to other atmospherically relevant types of INPs in the temperature range above 248 K. In the (high) Arctic, both transported dust and sea spray aerosol (transported or local) can be present (see Willis et al., 2018, for a thorough review of literature). However, which source is dominant for ice nucleation might be locally very different. In regions dominated by sea spray aerosol, the fraction of

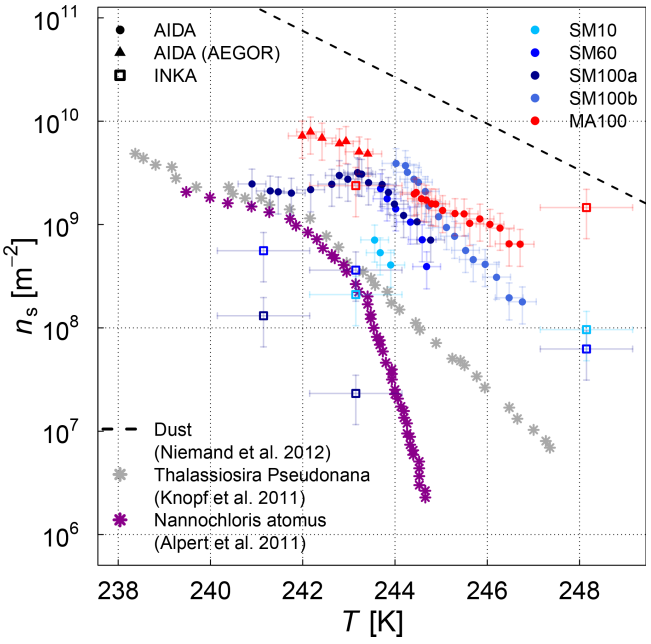

Figure 6. Surface-active-site density as a measure for ice nucleation activity at different temperatures for the two different diatom species (SM and MA) from the AIDA and INKA measurements. For SM, three samples grown under different nutrient regimes to generate cultures with different exudate properties (SM10, SM60, SM100) are shown. Literature n_s data for *Thalassiosira pseudonana* and *Nannochloris atomus* are shown as a comparison. The AIDA n_s data were corrected for the background ice nucleation mode observed in the reference experiments with purely inorganic Sigma-Aldrich sea salt solution droplets (see Sect. 2.4).

organic matter within the aerosol population is another uncertainty.

At low temperatures, the algal cultures had similar ice nucleation activities compared to the field samples, with *Melosira arctica* being slightly more ice active than *Skeletonema marinoi*. For *Skeletonema marinoi* grown under replete and deplete nutrient conditions, the culture with the highest nutrient limitation and inhibited growth (SM10) had somewhat lower n_s values compared to SM100 and SM60, but this trend is only distinct in the AIDA data and not as clearly visible in the INKA measurement. For comparison, we added previously published $n_s(T)$ values for two other algae: the diatom *Thalassiosira pseudonana* (Knopf et al., 2011) and the green algae *Nannochloris atomus* (Alpert et al., 2011a) (the data points were taken from Murray et al., 2012). The ice nucleation activities of these two species are in reasonable agreement with the data presented here. They lie towards the lower end of the AIDA data and fully overlap with the range of the n_s from the INKA measurements.

With respect to the comparison between the AIDA and INKA measurements, the INKA results tend to be shifted to lower n_s values, although the INKA data partly overlaps with the AIDA data within the respective error bars. As previous INP measurements for insoluble aerosol particles such as soil dust have shown good agreement between AIDA and INKA (DeMott et al., 2018a), the deviation for the current study with soluble, marine aerosol particles might be related to the particle phase state. For soluble aerosols, the different timescales and particle phase state evolution in the AIDA and INKA measurements might affect the observed INP data. In AIDA, the aerosol particles are initially suspended as aqueous solution droplets, gradually take up water when the expansion-cooling run is started, are activated to micrometre sized cloud droplets when the relative humidity exceeds 100 %, and potentially nucleate ice by immersion freezing upon further reduction of the temperature during expansion cooling. These processes occur on an overall timescale of approx. 5 min. For the INKA measurements, the aerosol particles are suspended as effloresced crystals in the APC chamber. During a very short time period of only 10 to 15 s in the first section of the CFDC chamber, the particles have to undergo the complex trajectory of deliquescence, droplet activation, and freezing. The short residence time in INKA might prevent equilibration of the aerosol to the instrument conditions. Thus, it is possible that at certain locations there is not enough water vapour present to fully activate the aerosol particles to cloud droplets, and this effect may account for the slightly lower n_s values compared to the AIDA measurements. Note that efflorescence might as well change the INP activity of the aerosol particles.

3.3 Combined bulk and aerosol phase measurements

One of the central aims of this study was to analyse the ice nucleation behaviour of Arctic SML samples and two different algal cultures over the full temperature range relevant for freezing in mixed-phase clouds. We also wanted to assess if the ice nucleation material is transferred from the bulk to the aerosol phase. The samples were measured with different instruments sensitive to different temperature regimes: AIDA and INKA below 248 K (aerosol phase) and µl-NIPI above 248 K (bulk). Here we attempt to directly compare the AIDA and µl-NIPI datasets. The INKA dataset is not included in the comparison since the AIDA dataset is more comprehensive and has a finer temperature resolution than the INKA data.

To enable comparison and to answer the question of whether the ice-nucleating material is transferred from the bulk to the aerosol phase, both datasets (AIDA and µl-NIPI) require normalization so that the ice nucleation behaviour can be expressed with the same quantity as a function of temperature. We have chosen to normalize both sets of data to the mass of salt present in the solution droplets since this quantity can be estimated for both approaches. Thus, the ice nucleation behaviour is expressed as ice nucleation active-site density per mass of salt (n_m, where the unit of n_m is per gram, g^{-1}). It is more obvious how to treat and harmonize ice nucleation data using materials like mineral dust, which has a relatively well-defined surface area. The surface area of an

aerosol dispersion can be used to derive n_s in much the same way as dust particles in bulk suspension. However, when the ice-nucleating material in a sample is soluble or forms colloidal suspensions, then it is less clear how to treat it. This is especially complex for the marine system, where the bulk sample can be very different from what is aerosolized into the atmosphere – one question that we want to investigate a bit further by comparing the AIDA and the µl-NIPI datasets. While we can (and have) derived n_s values for the AIDA and INKA data where the surface area is the surface area of the dry aerosol, we cannot do this for the bulk suspension measurements from the µl-NIPI instrument. Similarly, while we have a measure of organic mass for the bulk microlayer samples, we do not have a measurement of the organic mass in the aerosol phase; hence, we cannot normalize to organic mass. Solution volume cannot be used, since the volume of the solution of the aerosol changes as its concentration alters to come into equilibrium with the chamber conditions. Hence, we have chosen to normalize to the mass of salt, a quantity which can be readily estimated from both the bulk and aerosol experiments. When contrasting the resulting n_m values, it should be borne in mind that the spread in activities is likely an indication of the range of concentrations of the ice-active components as well as variability in the activity of those components. The objective of our work was to compare droplet-freezing assay results with aerosolized measurements rather than to derive a quantity which could be used to predict atmospheric INP. Ideally, we would quote active sites per unit mass of the nucleating component, but if the identity and mass of the nucleating component is unknown, this is not possible (as in this case). However, this approach enables us to investigate if the bulk and the aerosolized samples behave similarly and if both ice nucleation techniques complement each other when normalized and brought into one context.

For the µl-NIPI data, we derive the salt concentration for each sample (in $g\,L^{-1}$) using the measured water activity of the samples and the parameterization linking the water activity and salt concentration of seawater presented by Tang et al. (1997). To calculate the ice nucleation active-site density per mass of salt, the measured INP concentration (per litre) is simply divided by the salt concentration (in $g\,L^{-1}$). For the samples where no water activity was measured as part of this study (see Table 3), the values from Wilson et al. (2015) (for the ACCACIA SML samples) or an average of all SML samples (for the NETCARE STN samples) was used. We added an additional uncertainty of 20 % (arbitrary) to the error bars for the n_m values of the samples where the water activity was not directly measured. The ASCOS samples are not included in the unified dataset. Their water activity could not be directly measured because the remaining sample volume was too small. Furthermore, these samples were treated differently to the other microlayer samples so an average water activity might not be a good representation for these samples.

For the AIDA data, the measured FF was normalized with the measured mass concentration of dry particles (as obtained from the SMPS and APS measurements; see discussion in Sect. 2.2) instead of using the particle surface area concentration for normalization that yielded the n_s data shown in Figs. 5 and 6. The underlying assumption is that the dominating constituents in terms of mass is salt with a density of $2.017 \pm 0.006\,g\,cm^{-3}$ (Sigma-Aldrich sea salt; Zieger et al., 2017). Considering the composition of marine aerosols as presented in Gantt and Meskhidze (2013), this assumption is fair for the typical sizes of aerosol particles aerosolized for the AIDA.

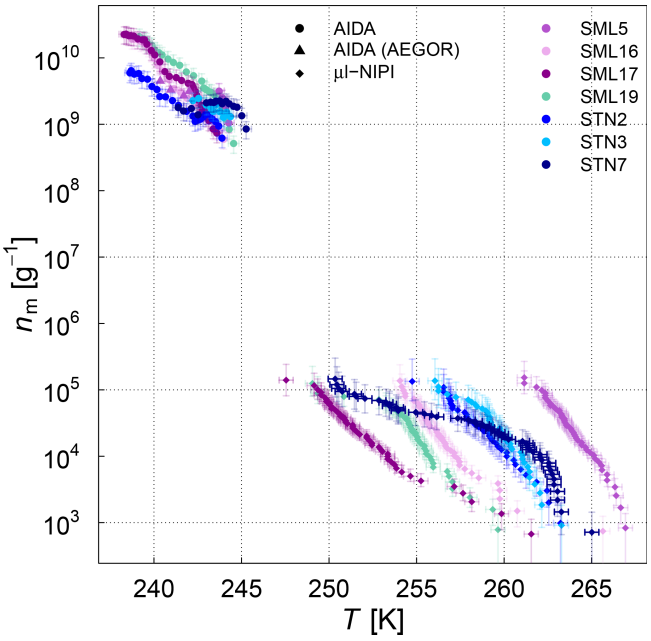

Figure 7. Normalized AIDA and µl-NIPI measurements for 7 field samples showing a full ice nucleation spectrum represented as ice nucleation active-site density per mass of sea salt (n_m). For the AIDA measurements, both aerosolization techniques (nebulizer and AEGOR) are included. The points of the µl-NIPI measurements which could have been affected by background signal and represent upper limits are indicated by a lower error bar that is unchanged from the previous point, as there may have been no additional INP detected above the background signal. The temperature in this plot was corrected for freezing-point depression caused by salts for the µl-NIPI measurements.

INP transfer from the bulk to the aerosol phase

The combined ice nucleation activity of the field samples are shown in Fig. 7. The combined temperature spectra for the ice nucleation activity of the algal samples is shown in Figs. 8 and 9; the samples were split into two figures for clarity.

We first turn to the comparison between the AIDA and µl-NIPI measurements for the algal and field samples focusing on the difference between aerosolized and bulk samples. A significant difference between the AIDA and µl-NIPI measurements is that one is derived from an aerosolized sample

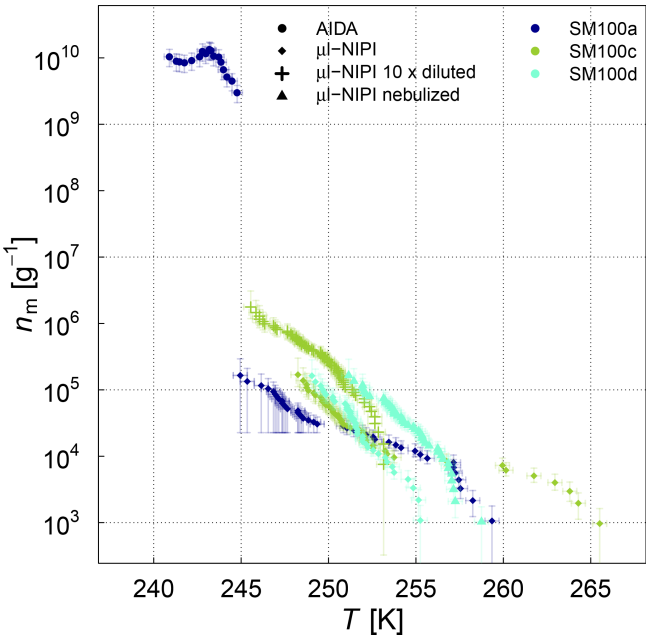

Figure 8. Ice nucleation active-site density per mass of sea salt (n_m) estimated from the AIDA and µl-NIPI measurements for the SM100 culture samples. For the µl-NIPI measurements, the SM100 samples were additionally diluted with ultrapure water. Note that the dilution was conducted up to 8 weeks after the main campaign (Leeds, UK). The points of the µl-NIPI measurements which could have been affected by the background signal and represent upper limits are indicated by the lower error bar unchanged from the previous point, as there may have been no additional INP detected above the background signal. The temperature in this plot was corrected for freezing-point depression caused by salts for the µl-NIPI measurements.

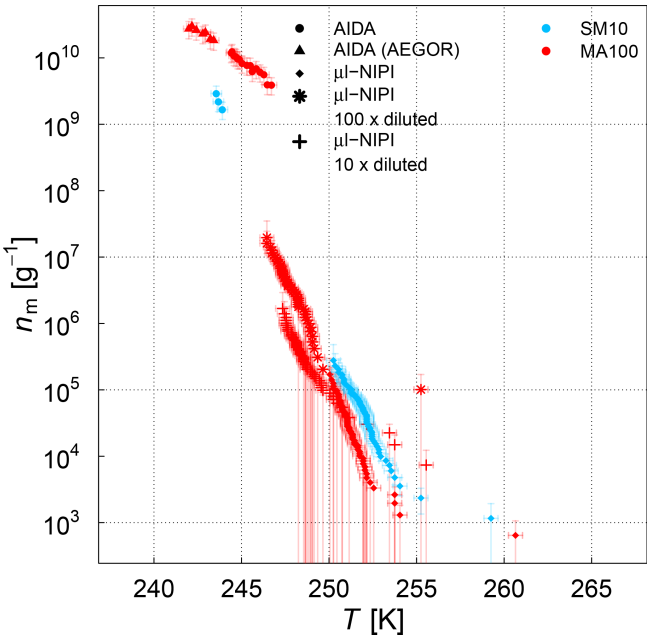

Figure 9. Ice nucleation active-site density per mass of sea salt (n_m) estimated from the AIDA and µl-NIPI measurements for the SM10 and MA culture samples. For the AIDA measurements, both aerosolization techniques (nebulizer and AEGOR) are included. For the µl-NIPI measurements, the MA100 sample was additionally diluted with ultrapure water. Note that the dilution was conducted up to 8 weeks after the main campaign (Leeds, UK). The points of the µl-NIPI measurements which could have been affected by background signal and represent upper limits are indicated by the lower error bar unchanged from the previous point, as there may have been no additional INP detected above the background signal. The temperature in this plot was corrected for freezing-point depression caused by salts for the µl-NIPI measurements.

and one is derived directly from the pipetted culture medium. Comparison between µl-NIPI, AIDA, and other instruments in a recent intercomparison was very good (DeMott et al., 2018b). Inspection of the data in Figs. 7, 8, and 9 suggests that the data from the two techniques might be consistent, but n_m would have to be extremely steep at the intermediate temperatures. The discontinuity of the AIDA and the NIPI data; i.e. the shift of the AIDA data to higher n_m values, might be related to a change of physical characteristics upon aerosolization. Aerosolization may alter the physical characteristics of the ice-nucleating material compared to when it is in the culture medium through breaking up aggregates or disrupting cells. This was shown for *Pseudomonas syringae* cells in the study of Alsved et al. (2018). Hence, it is feasible that the ice nucleation activities of the aerosolized samples in the AIDA experiments are higher than those in the µl-NIPI experiments. However, there is a recognizable difference between both types of samples. The aerosolization technique might exert more of an influence on the cultured samples compared to the microlayer samples, where the INP are thought to be associated with submicron organic detritus rather than intact cells. For the SML samples, it is therefore reasonable to assume that the composition of the aerosolized solution droplets probed in the AIDA chamber is very similar to that of the corresponding bulk solutions used in the µl-NIPI measurements. Indeed, the n_m spectrum looks more uniform compared to the algal cultures. Most samples feature a rather continuous slope in the temperature-dependent INP spectrum. One notable exception is the STN7 sample, which shows a pronounced stepwise change in the ice nucleation behaviour at about 263 K.

For the algal cultures, the assumption that the aerosolized and bulk samples are similar is not necessarily valid. In order to investigate if the process of nebulizing influences the ice-nucleating activity of cell suspensions, we nebulized a SM100 sample, collected the nebulized sample as a bulk liquid, and retested its ice-nucleating activity using the µl-NIPI. Nebulization increased the activity of the sample (see Fig. 3b). We suggest that this might be consistent with the break up or rupture of cells in the vigorous nebulization process, which might then release macromolecu-

lar ice-nucleating material. Alternatively, there might be agglomerated cells or colloidal particles inside the sample. That means that ice-active sites can be either inaccessible or simply concentrated on a few particles. These aggregates might remain relatively intact during pipetting but may be disrupted on nebulization. It would have the effect of dispersing the ice-nucleating entities throughout the aqueous suspension and thus increasing the probability of freezing across the droplet distribution when nebulizing the sample. However, nebulizing Milli-Q water (not shown) showed that some impurities can likely be introduced by the nebulizer itself. These hypotheses deserve further investigation in the future.

Furthermore, we have the hypothesis that the aerosolized material entering AIDA was very different compared to the pure cultures. For example, first analysis of electron micrograms of aerosol particles contained in AIDA (representative for particles aerosolized with a nebulizer for AIDA) during the experiments with *Skeletonema marinoi* showed no cells or obvious cell fragments visible (see Fig. 10a). This is consistent with the microlayer being dominantly composed of organic detritus and might be a result of biochemical processes within the microlayer. In contrast, Fig. 10b, where SM100 droplets were pipetted directly from the solution, clearly shows cells, which are then also present in the droplets analysed with µl-NIPI. However, a more detailed analysis would be needed to give a final answer on the difference of the aerosol particles in AIDA compared with aerosol particles within pipetted droplets.

Dilution tests bulk measurements

Figure 8 shows the $n_m(T)$ spectra for the SM100 culture and the variability including two SM100 samples (a and b for biological variability; c and d for storage effects) as discussed in Sect. 3.1. The latter (Fig. 9) shows the spectra for MA100 and SM10. To bridge the gap in the ice nucleation spectra between the AIDA and the µl-NIPI data, we did additional dilution experiments with µl-NIPI to extend the temperature regime of the µl-NIPI data to lower temperatures. Diluting the SM100 and MA100 sample has the effect of reducing the freezing temperature and increasing n_m. Thus the curves from the undiluted samples can be extended to lower temperatures. That works well for SM100 and partly also for MA100. For MA100, the slope of the n_m curve continues to be steep throughout the dilutions. However, there are some points which may have been affected by the background signal, which are denoted by the larger lower-error-bar value. It is not clear why there is such a difference in the behaviour after dilution between the SM100 and MA100 samples, and further investigation into the differences in their composition and how this is related to their ice-nucleating ability is necessary.

Temperature-dependent difference in ice nucleation behaviour

As a striking result, there is much more variability in the ice nucleation activity of the samples when analysed with the µl-NIPI than with AIDA (approx. 15 K vs. 5 K). This larger variability in the high-temperature range has been observed in other studies, too (e.g. for soil or agricultural dust; O'Sullivan et al., 2014; Schiebel, 2017; Suski et al., 2018). One explanation for this behaviour could be that there are multiple INP types in seawater, just like there are in terrestrial samples, leading to a high diversity of the INP spectra at high temperatures. At low temperature the ice nucleation activity is much less variable and low throughout all samples.

4 Conclusions

In this study the ice nucleation activity of several bulk and aerosolized SML samples from the Arctic region was investigated and compared with pure and aerosolized samples of two diatom cultures (*Skeletonema marinoi* and *Melosira arctica*). The measurements were conducted with a suite of ice nucleation instruments (AIDA, INKA, µl-NIPI) which are sensitive in different temperature regimes across the whole mixed-phase cloud temperature range (below and above 248 K). In order to compare the different approaches and the ability of the ice-nucleating material to transfer to the aerosol phase, we have normalized all of the measurements by the salt mass present in the bulk and aerosolized samples. Normalization in this manner results in an ice nucleation active-site density per mass of salt n_m.

Our three main objectives were the following: first, the comparison of the ice-nucleating ability of two common phytoplankton species with Arctic microlayer samples; second, the impact of the aerosolization technique on the results; and third, the sample variability over the entire mixed-phase cloud temperature range. Concerning these objectives we can draw the following conclusions.

When comparing the full temperature spectrum of the algal cultures with the field samples, it is evident that the culture samples are similar to the field samples in the low-temperature regime but are not among the most ice-active samples of the spectrum in the high-temperature regime. As the investigated algal species show less ice activity in the temperature regime above 248 K compared to the natural field samples, we conclude that they, especially *Melosira arctica*, cannot explain the freezing at the high temperatures. A normalization of the samples to the atmospheric algal content would be needed to quantify this observation. This result indicates that the INPs active at the highest temperatures are not one of the two types of phytoplankton cells studied or their exudates. However, since we have only tested two mono-species grown axenically and harvested in the exponential growth phase, we cannot rule out ice nucleation being

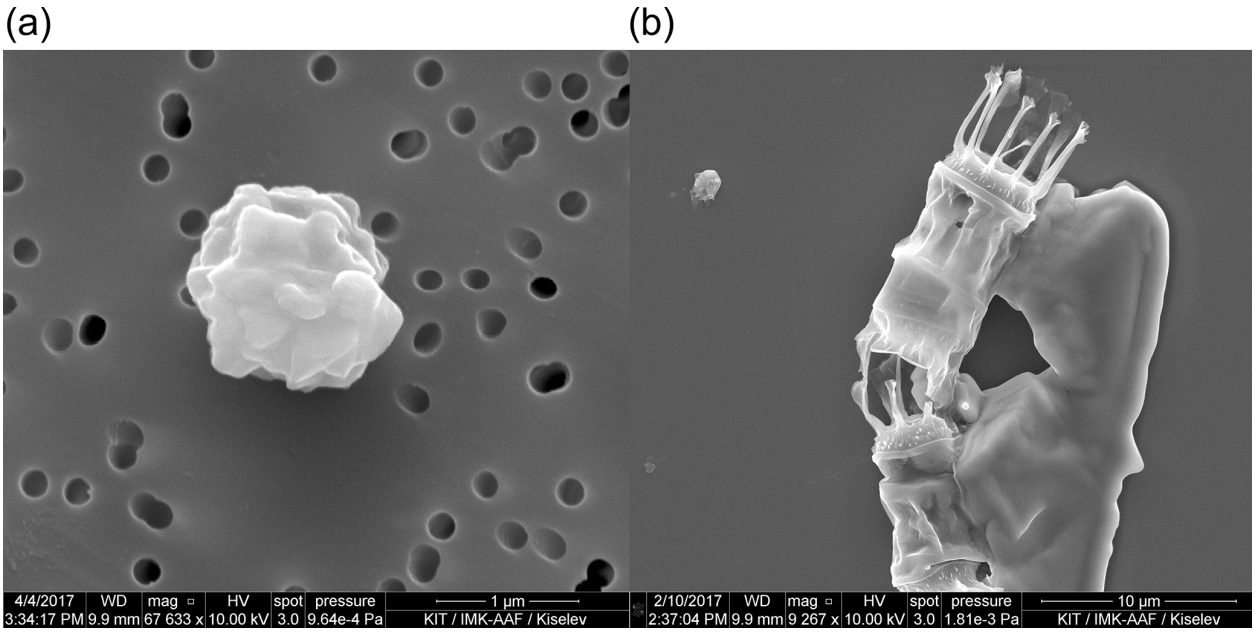

Figure 10. Electron microscope images of SM10 (aerosolized by AEGOR) collected from AIDA **(a)** and SM100 in droplets pipetted directly from the solution **(b)**.

triggered by a consortia of microorganisms facilitating break-up of cells and a mass release of organic matter from a phytoplankton bloom. The freshly produced pure algal cultures are different from the diluted field samples, which are highly diverse in terms of composition. Aged algal cultures may exhibit a different freezing behaviour. For *Skeletonema marinoi*, the culture was grown at different nutrition conditions to test the dependence of the freezing on the algal characteristics, such as total organic carbon (cell organic carbon and all dissolved organic carbon), cell wall structure, colony length etc. No significant difference could be found when comparing the ice nucleation behaviour of the samples grown at different rates and under varying nutrient limitation, so there is no clear evidence for a correlation between the total organic carbon content of the culture sample (see Table 3) and the freezing of the sample.

A key aspect of this study is that we have used both a sea spray simulation chamber and a nebulizer to introduce samples into AIDA (low temperature regime). Using a sea spray simulation chamber (AEGOR) allowed us to test the effect of mimicking the process of bubble bursting on the ice activity of the aerosol generated. A larger spread was observed in general for the SML samples diluted in AEGOR – some retained the activity of the undiluted sample and in some cases the IN ability decreased below the detection limit. Lower ice nucleation active-site densities (for the cases where the IN ability decreased below the detection limit) can be explained by the difference in the size distribution of the aerosols generated by the two approaches.

When analysing the ice nucleation spectra over the whole temperature regime, it was seen that the SML field samples exhibit a high variability in ice nucleation activity in the temperature regime above 248 K compared with lower temperatures. Above 248 K the variation in the median freezing temperature, T_{50}, is approx. 15 K with some samples showing a strong freezing signal at high temperatures ($T_{50} \approx 262$ K), while below 248 K the spread of T_{50} is only approx. 5 K. The behaviour of the samples in the different temperature regimes might be related to different types of INPs active in the different regimes. In the temperature range below 248 K, the results of this study are in the upper range of the values measured by DeMott et al. (2016), which show a larger spread compared to the results of the nebulized samples. This larger spread could be explained by the aerosolization (see paragraph above). However, neither the SML nor the algal samples exhibit a strong freezing signal in the low-temperature regime (below 248 K) compared to desert dust. There was no significant freezing above the detection limit in the AIDA chamber (around 2×10^8 m^{-2}) at temperatures higher than 246 K. The ice nucleation active-surface-site densities were generally at least 1 order of magnitude lower than those for desert dust.

We also tentatively show that nebulization enhances the ice-nucleating ability of some cell cultures. We suggest that the aerosolization process using a nebulizer might rupture individual cells allowing ice-nucleating macromolecules to be dispersed through the aerosol population. Alternatively aggregates of cells or colloidal material may be broken up during aerosolization. This might be unlikely to be rele-

vant for environmental conditions. Here, this may lead to the aerosolized samples in the AIDA chamber having a greater ice-nucleating activity than they would otherwise have. Pipetting of droplets, as done for the µl-NIPI measurements, might be much less likely to exert sufficient force on the samples to break up cells, aggregates, or colloidal material. Our hypothesis is that this process is particularly important for cell cultures and is less important in microlayer samples which consist of organic "detritus" rather than intact cells (i.e. the organic material is already well dispersed).

In the experiments with microlitre volume droplets (µl-NIPI), which are sensitive to rarer ice-nucleating particles, some of the SML samples have values of $T_{50} \approx 262$ K. This indicates that there is a low concentration of relatively active ice-nucleating entities in these samples. The high variability observed in the high-temperature regime suggests that there is a substantial variability in the presence of INP in the samples. What gives rise to this variability and what factors control it are particularly important outstanding questions. Previous work has shown that both the type and concentration of INP vary substantially throughout the development and decay of a phytoplankton bloom (Wang et al., 2015; McCluskey et al., 2017; Wilbourn et al., 2020). There are perhaps various types of marine INPs from different biological sources present in these natural samples. While our results (and those in the literature, e.g. Knopf et al., 2011 and Alpert et al., 2011a), show that phytoplankton can nucleate ice, it is also feasible that bacteria exploiting organic detritus from a plume might nucleate ice (Fall and Schnell, 1985). The presence of bacterial proteinaceous ice-nucleating material would be consistent with the observation that INPs in microlayer samples are heat sensitive (e.g. Wilson et al., 2015 and Irish et al., 2017). However, a heat treatment test (see Appendix) on SM100 did not give a clear indication for this hypothesis: in the low-temperature regime there was no heat sensitivity of freezing, but a significant deactivation of freezing on heating could be seen in the high-temperature regime for that sample. Since bacteria tend to be larger than 200 nm and bacterial ice-active proteins are cell-membrane bound, one would expect to lose the ice activity associated with bacteria when filtering the sample through a 0.2 µm filter (Maki et al., 1974; Murray et al., 2012). This could not be seen in our results of the differently treated ASCOS samples, where the filtered ASCOS sample < 0.22 µm did not show any reduction in ice nucleation activity. The ice nucleation activity of this sample indicated that macromolecules are responsible for the freezing, which were highly concentrated in the sample. It was suggested in the literature that marine INPs are very small and heat sensitive (Schnell and Vali, 1975; Vali et al., 1976; Wilson et al., 2015; Irish et al., 2017, 2019b), which is consistent with an ice-nucleating protein responsible for the INP activity, similar to those found in terrestrial fungi (Pouleur et al., 1992; O'Sullivan et al., 2015, 2016). Marine viruses may also fit this size requirement, although we are not aware of any studies on them for ice nucleation. A different candidate could be bacterial vesicles which are $\sim$ 50–200 nm particles and can retain the ice-nucleating activity of their parent bacterium (Phelps et al., 1986). Another possibility is that the ice-nucleating ability of the organic material in seawater is in part due to riverine input. River water is known to harbour large quantities of macromolecular INPs (Larsen et al., 2017; Moffett et al., 2018), and the observed anticorrelation between INPs and salinity is consistent with a significant riverine input of INPs to some marine environments (Irish et al., 2019b). Given the massive diversity of the high-temperature INPs observed in seawater in this and previous studies (e.g. Schnell and Vali, 1975; Schnell, 1977; Wilson et al., 2015; Irish et al., 2017, 2019b), it is likely that the sources of these INPs are also highly variable and heterogeneous, much as they are in the terrestrial environment.

From our study it is difficult to answer the questions of whether Arctic regions may have local marine sources of INPs and how much they influence Arctic mixed-phase clouds. At temperatures above 248 K the ice nucleation activity of the investigated samples was very diverse, with some samples reaching a quite high median freezing temperature of 262 K, and thus potentially being able to trigger freezing in Arctic mixed-phase clouds. The measurements in the temperature regime below 248 K, on the other hand, did not show that the samples were particularly ice active, especially when compared to dust, despite the fact that the results show an upper limit for n_s. Both measurements differed in the way the samples were analysed (bulk vs. aerosol phase). This was most relevant for the cultured samples, giving some hint that aerosolization of cell cultures may change the ice nucleation activity of these, which is a process that could be important in the environment as well.

Appendix A: Heat test SM100

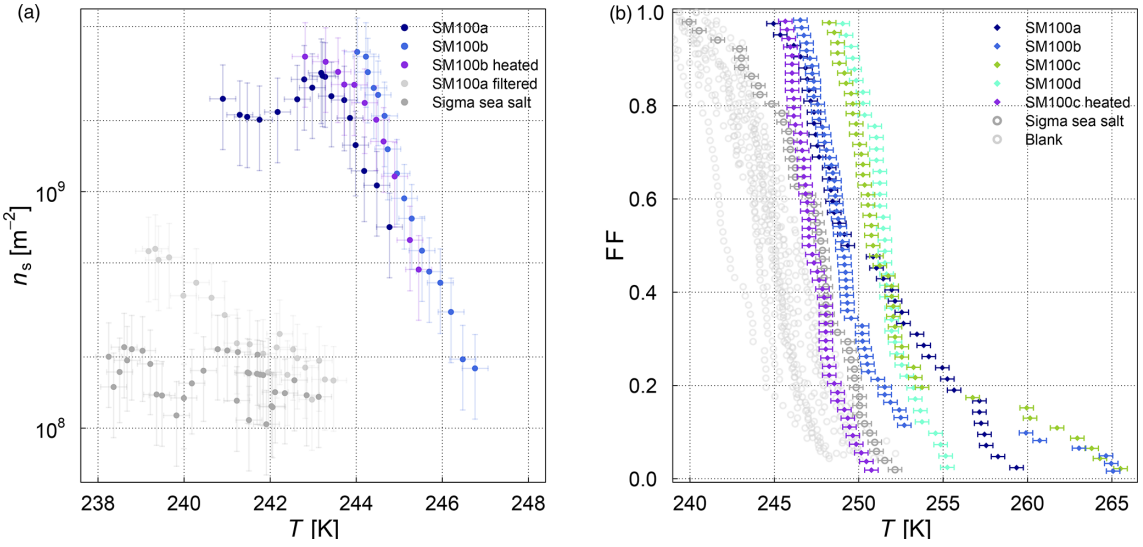

Figure A1. Heat test of SM100 measured with **(a)** AIDA (surface-active-site density n_s as a measure for ice nucleation activity at different temperatures) and **(b)** µl-NIPI (fraction frozen curve). The temperature in the µl-NIPI plot was corrected for freezing-point depression caused by salts.

Code and data availability. The data are available at the KITopen data repository (https://www.bibliothek.kit.edu/cms/kitopen.php, last access: 23 September 2020) under the following https://doi.org/10.5445/IR/1000122595 (Ickes et al., 2020).

Author contributions. MES and RW were responsible for the conceptualization and the overall lead of the measurement campaign. During the measurement campaign, RW and LI were conducting the AIDA measurements, GCEP and MPA the µl-NIPI measurements, SB and KH the INKA measurements, SC the CCN measurements, and AAK and LI the filter sampling for electron microscopy. EG did culture the algal samples, GCEP provided the SML samples, and CL the ASCOS samples. The AIDA data were analyzed by LI, RU, and RW; the µl-NIPI data by GCEP and MPA; the INKA data by SB, KH, and TS; the CCN data by SC; and the electron microscopy was done by AAK. The figures were done by LI except Fig. 10, which was produced by AAK. Figure 1 was done with contributions from MES. The article was written by LI, MES, RW, KH, BJM, and GCEP. All authors contributed in reviewing and editing of the article.

Competing interests. The authors declare that they have no conflict of interest.

Acknowledgements. We gratefully acknowledge the support of the Engineering and Infrastructure group of IMK-AAF, especially Olga Dombrowski, Rainer Buschbacher, Tomasz Chudy, Steffen Vogt, and Georg Scheurig. We thank Victoria E. Irish for shipment and help with the SML samples (STN). We thank Nadine Hoffmann (IMK-AAF) for preparing the SM samples for the ESEM measurements. We thank the two anonymous reviewers for valuable feedback.

Financial support. This study was supported by the Helmholtz-Gemeinschaft Deutscher Forschungszentren as part of the programme "Atmosphere and Climate". We thank EUROCHAMP-2020 for TNA (Trans-national Access) support and funding and the Bolin Centre for Climate Research for supporting our data workshop held in Stockholm in 2017. Luisa Ickes was supported by the Swiss National Science Foundation (Early Postdoc.Mobility) and the Swedish Science Foundation (Vetenskapsrådet) with grant no. 2015-05318. Matthew E. Salter was supported by the Swedish Science Foundation (Vetenskapsrådet) with grant no. 2016-05100. Caroline Leck was supported by the Swedish Science Foundation (Vetenskapsrådet) with grant no. 2016-03518. Benjamin J. Murray, Grace C. E. Porter, and Michael P. Adams were supported by the European Research Council under the Horizon 2020 research and innovation programme (MarineIce (grant no. 648661)), Merete Bilde and Sigurd Christiansen were supported by Aarhus University and Hakon Lund Foundation, and Allan K. Bertram was supported by the Natural Sciences and Engineering Research Council of Canada with funding.

The article processing charges for this open-access publication were covered by Stockholm University.

Review statement. This paper was edited by Markus Petters and reviewed by two anonymous referees.

References

Alpert, P. A., Aller, J. Y., and Knopf, D. A.: Initiation of the ice phase by marine biogenic surfaces in supersaturated gas and supercooled aqueous phases, Phys. Chem. Chem. Phys., 13, 19882–19894, https://doi.org/10.1039/C1CP21844A, 2011a.

Alpert, P. A., Aller, J. Y., and Knopf, D. A.: Ice nucleation from aqueous NaCl droplets with and without marine diatoms, Atmos. Chem. Phys., 11, 5539–5555, https://doi.org/10.5194/acp-11-5539-2011, 2011b.

Alpert, P. A., Kilthau, W. P., Bothe, D. W., Radway, J. C., Aller, J. Y., and Knopf, D. A.: The influence of marine microbial activities on aerosol production: A laboratory mesocosm study, J. Geophys. Res.-Atmos., 120, 8841–8860, https://doi.org/10.1002/2015JD023469, 2015.

Alsved, M., Holm, S., Christiansen, S., Smidt, M., Rosati, B., Ling, M., Boesen, T., Finster, K., Bilde, M., Löndahl, J., and Šantl Temkiv, T.: Effect of Aerosolization and Drying on the Viability of Pseudomonas syringae Cells, Front. Microbiol., 9, 3086, https://doi.org/10.3389/fmicb.2018.03086, 2018.

Battan, L. J. and Riley, J. J.: Ice-crystal nuclei and maritime air, J. Meteorol., 17, 675–676, 1960.

Benz, S., Megahed, K., Möhler, O., Saathoff, H., Wagner, R., and Schurath, U.: T-dependent rate measurements of homogeneous ice nucleation in cloud droplets using a large atmospheric simulation chamber, J. Photoch. Photobio. A, 176, 208–217, https://doi.org/10.1016/j.jphotochem.2005.08.026, 2005.

Bigg, E. K.: A new Technique for Counting Ice-Forming Nuclei in Aerosols, Tellus, 9, 394–400, https://doi.org/10.1111/j.2153-3490.1957.tb01895.x, 1957.

Bigg, E. K.: Ice nucleus concentrations in remote areas, J. Atmos. Sci., 30, 1153–1157, 1973.

Bigg, E. K.: Long-term trends in ice nucleus concentrations, Atmos. Res., 25, 409–415, 1990.

Bigg, E. K.: Ice forming nuclei in the high Arctic, Tellus B, 48, 223–233, 1996.

Bigg, E. K., Mossop, S. C., Meade, R. T., and Thorndike, N. S. C.: The measurement of ice nucleus concentrations by means of Millipore filters, J. Appl. Meteorol., 2, 266–269, 1963.

Birstein, S. J. and Anderson, C. E.: Preliminary report on sea salt as an ice nucleus, J. Meteorol., 10, 166–166, 1953.

Booth, B. C. and Horner, R. A.: Microalgae on the arctic ocean section, 1994: species abundance and biomass, Deep-Sea Res. Pt. II, 44, 1607–1622, https://doi.org/10.1016/S0967-0645(97)00057-X, 1997.

Borkman, D. G. and Smayda, T.: Multidecadal (1959–1997) changes in Skeletonema abundance and seasonal bloom patterns in Narragansett Bay, Rhode Island, USA, J. Sea Res., 61, 84–94, https://doi.org/10.1016/j.seares.2008.10.004, 2009.

Borys, R. D.: Studies of ice nucleation by arctic aerosol on AGASP-II, J. Atmos. Chem., 9, 169–185, 1989.

Borys, R. D. and Grant, L. O.: The Effects of long-range transport of air pollutants on Arctic cloud-active aerosol, PhD thesis, Colorado State University, Atmospheric Science Paper No. 367, 339 pp., 1983.

Boucher, O., Randall, D., Artaxo, P., Bretherton, C., Feingold, G., Forster, P., Kerminen, V.-M., Kondo, Y., Liao, H., Lohmann, U., Rasch, P., Satheesh, S. K., Sherwood, S., Stevens, B., and Zhang, X. Y.: Clouds and Aerosols, in: Climate Change 2013: The Physical Science Basis. Contribution of Working Group I to the Fifth Assessment Report of the Intergovernmental Panel on Climate Change, edited by: Stocker, T. F., Qin, D., Plattner, G.-K., Tignor, M., Allen, S. K., Boschung, J., Nauels, A., Xia, Y., Bex, V., and Midgley, P. M., Cambridge University Press, Cambridge, United Kingdom and New York, NY, USA, 2013.

Brier, G. W. and Kline, D. B.: Ocean water as a source of ice nuclei, Science, 130, 717–718, 1959.

Burrows, S. M., Hoose, C., Pöschl, U., and Lawrence, M. G.: Ice nuclei in marine air: biogenic particles or dust?, Atmos. Chem. Phys., 13, 245–267, https://doi.org/10.5194/acp-13-245-2013, 2013.

Canesi, K. L. and Rynearson, T. A.: Temporal variation of Skeletonema community composition from a long-term time series in Narragansett Bay identified using high-throughput DNA sequencing, Mar. Ecol.-Prog. Ser., 556, 1–16, https://doi.org/10.3354/meps11843, 2016.

Chahine, M. T.: The hydrological cycle and its influence on climate, Nature, 359, 373–380, 1992.

Christiansen, S., Salter, M. E., Gorokhova, E., Nguyen, Q. T., and Bilde, M.: Sea Spray Aerosol Formation: Laboratory Results on the Role of Air Entrainment, Water Temperature, and Phytoplankton Biomass, Environ. Sci. Technol., 53, 13107–13116, 2019.

Christiansen, S., Ickes, L., Bulatovic, I., Leck, C., Murray, B. J., Bertram, A. K., Wagner, R., Gorokhova, E., Salter, M. E., Ekman, A. M. L., and Bilde, M.: Influence of Arctic microlayers and algal cultures on sea spray hygroscopicity and the possible implications for mixed-phase clouds, J. Geophys. Res.-Atmos., 125, e2020JD032808, https://doi.org/10.1029/2020JD032808, 2020.

Collins, D. B., Zhao, D. F., Ruppel, M. J., Laskina, O., Grandquist, J. R., Modini, R. L., Stokes, M. D., Russell, L. M., Bertram, T. H., Grassian, V. H., Deane, G. B., and Prather, K. A.: Direct aerosol chemical composition measurements to evaluate the physicochemical differences between controlled sea spray aerosol generation schemes, Atmos. Meas. Tech., 7, 3667–3683, https://doi.org/10.5194/amt-7-3667-2014, 2014.

Creamean, J. M., Kirpes, R. M., Pratt, K. A., Spada, N. J., Maahn, M., de Boer, G., Schnell, R. C., and China, S.: Marine and terrestrial influences on ice nucleating particles during continuous springtime measurements in an Arctic oilfield location, Atmos. Chem. Phys., 18, 18023–18042, https://doi.org/10.5194/acp-18-18023-2018, 2018.

Creamean, J. M., Cross, J. N., Pickart, R., McRaven, L., Lin, P., Pacini, A., Hanlon, R., Schmale, D. G., Ceniceros, J., Aydell, T., Colombi, N., Bolger, E., and DeMott, P. J.: Ice Nucleating Particles Carried From Below a Phytoplankton Bloom to the Arctic Atmosphere, Geophys. Res. Lett., 46, 8572–8581, https://doi.org/10.1029/2019GL083039, 2019.

DeMott, P. J., Prenni, A. J., Liu, X., Kreidenweis, S. M., Petters, M. D., Twohy, C. H., Richardson, M. S., Eidhammer, T., and Rogers, D. C.: Predicting global atmospheric ice nuclei distributions and their impacts on climate, P. Natl. Acad. Sci. USA, 107, 11217–11222, 2010.

DeMott, P. J., Hill, T. C. J., McCluskey, C. S., Prather, K. A., Collins, D. B., Sullivan, R. C., Ruppel, M. J., Mason, R. H., Irish, V. E., Lee, T., Hwang, C. Y., Rhee, T. S., Snider, J. R., McMeeking, G. R., Dhaniyala, S., Lewis, E. R., Wentzell, J. J. B., Abbatt, J., Lee, C., Sultana, C. M., Ault, A. P., Axson, J. L., Diaz Martinez, M., Venero, I., Santos-Figueroa, G., Stokes, M. D., Deane, G. B., Mayol-Bracero, O. L., Grassian, V. H., Bertram, T. H., Bertram, A. K., Moffett, B. F., and Franc, G. D.: Sea spray aerosol as a unique source of ice nucleating particles, P. Natl. Acad. Sci. USA, 113, 5797–5803, https://doi.org/10.1073/pnas.1514034112, 2016.

DeMott, P. J., Mason, R. H., McCluskey, C. S., Hill, T. C. J., Perkins, R. J., Desyaterik, Y., Bertram, A. K., Trueblood, J. V., Grassian, V. H., Qiu, Y., Molinero, V., Tobo, Y., Sultana, C. M., Lee, C., and Prather, K. A.: Ice nucleation by particles containing long-chain fatty acids of relevance to freezing by sea spray aerosols, Environ. Sci.: Processes Impacts, 20, 1559–1569, https://doi.org/10.1039/C8EM00386F, 2018a.

DeMott, P. J., Möhler, O., Cziczo, D. J., Hiranuma, N., Petters, M. D., Petters, S. S., Belosi, F., Bingemer, H. G., Brooks, S. D., Budke, C., Burkert-Kohn, M., Collier, K. N., Danielczok, A., Eppers, O., Felgitsch, L., Garimella, S., Grothe, H., Herenz, P., Hill, T. C. J., Höhler, K., Kanji, Z. A., Kiselev, A., Koop, T., Kristensen, T. B., Krüger, K., Kulkarni, G., Levin, E. J. T., Murray, B. J., Nicosia, A., O'Sullivan, D., Peckhaus, A., Polen, M. J., Price, H. C., Reicher, N., Rothenberg, D. A., Rudich, Y., Santachiara, G., Schiebel, T., Schrod, J., Seifried, T. M., Stratmann, F., Sullivan, R. C., Suski, K. J., Szakáll, M., Taylor, H. P., Ullrich, R., Vergara-Temprado, J., Wagner, R., Whale, T. F., Weber, D., Welti, A., Wilson, T. W., Wolf, M. J., and Zenker, J.: The Fifth International Workshop on Ice Nucleation phase 2 (FIN-02): laboratory intercomparison of ice nucleation measurements, Atmos. Meas. Tech., 11, 6231–6257, https://doi.org/10.5194/amt-11-6231-2018, 2018b.

Fahey, D. W., Gao, R.-S., Möhler, O., Saathoff, H., Schiller, C., Ebert, V., Krämer, M., Peter, T., Amarouche, N., Avallone, L. M., Bauer, R., Bozóki, Z., Christensen, L. E., Davis, S. M., Durry, G., Dyroff, C., Herman, R. L., Hunsmann, S., Khaykin, S. M., Mackrodt, P., Meyer, J., Smith, J. B., Spelten, N., Troy, R. F., Vömel, H., Wagner, S., and Wienhold, F. G.: The AquaVIT-1 intercomparison of atmospheric water vapor measurement techniques, Atmos. Meas. Tech., 7, 3177–3213, https://doi.org/10.5194/amt-7-3177-2014, 2014.

Fall, R. and Schnell, R. C.: Association of an ice-nucleating pseudomonad with cultures of the marine dinoflagellate, Heterocapsa niei, J. Mar. Res., 43, 257–265, https://doi.org/10.1357/002224085788437370, 1985.

Flyger, H. and Heidam, N. Z.: Ground level measurements of the summer tropospheric aerosol in Northern Greenland, J. Aerosol Sci., 9, 157–168, https://doi.org/10.1016/0021-8502(78)90075-7, 1978.

Fountain, A. G. and Ohtake, T.: Concentrations and source areas of ice nuclei in the Alaskan atmosphere, J. Clim. Appl. Meteorol., 24, 377–382, 1985.

Gagin, A. and Arroyo, M.: A thermal diffusion chamber for the measurement of ice nucleus concentration, J. Rech. Atmos., 55, 115–122, 1969.

Gantt, B. and Meskhidze, N.: The physical and chemical characteristics of marine primary organic aerosol: a review, At-

mos. Chem. Phys., 13, 3979–3996, https://doi.org/10.5194/acp-13-3979-2013, 2013.

Gao, Q., Leck, C., Rauschenberg, C., and Matrai, P. A.: On the chemical dynamics of extracellular polysaccharides in the high Arctic surface microlayer, Ocean Sci., 8, 401–418, https://doi.org/10.5194/os-8-401-2012, 2012.

Garrett, T. J., Maestas, M. M., Krueger, S. K., and Schmidt, C. T.: Acceleration by aerosol of a radiative-thermodynamic cloud feedback influencing Arctic surface warming, Geophys. Res. Lett., 36, L19804, https://doi.org/10.1029/2009GL040195, 2009.

Gong, X., Wex, H., Müller, T., Wiedensohler, A., Höhler, K., Kandler, K., Ma, N., Dietel, B., Schiebel, T., Möhler, O., and Stratmann, F.: Characterization of aerosol properties at Cyprus, focusing on cloud condensation nuclei and ice-nucleating particles, Atmos. Chem. Phys., 19, 10883–10900, https://doi.org/10.5194/acp-19-10883-2019, 2019.

Gong, X., Wex, H., van Pinxteren, M., Triesch, N., Fomba, K. W., Lubitz, J., Stolle, C., Robinson, T.-B., Müller, T., Herrmann, H., and Stratmann, F.: Characterization of aerosol particles at Cabo Verde close to sea level and at the cloud level – Part 2: Ice-nucleating particles in air, cloud and seawater, Atmos. Chem. Phys., 20, 1451–1468, https://doi.org/10.5194/acp-20-1451-2020, 2020.

Hartmann, M., Adachi, K., Eppers, O., Haas, C., Herber, A., Holzinger, R., Hünerbein, A., Jäkel, E., Jentzsch, C., van Pinxteren, M., Wex, H., Willmes, S., and Stratmann, F.: Wintertime Airborne Measurements of Ice Nucleating Particles in the High Arctic: A Hint to a Marine, Biogenic Source for Ice Nucleating Particles, Geophys. Res. Lett., 47, e2020GL087770, https://doi.org/10.1029/2020GL087770, 2020.

Harvey, G. W.: Microlayer collection from the sea surface: a new method and initial results, Limnol. Oceanogr., 11, 608–613, https://doi.org/10.4319/lo.1966.11.4.0608, 1966.

Henderson, R., Chips, M., Cornwell, N., Hitchins, P., Holden, B., Hurley, S., Parsons, S. A., Wetherill, A., and Jefferson, B.: Experiences of algae in UK waters: a treatment perspective, Water Environ. J., 22, 184–192, https://doi.org/10.1111/j.1747-6593.2007.00100.x, 2008.

Herbert, R. J., Murray, B. J., Whale, T. F., Dobbie, S. J., and Atkinson, J. D.: Representing time-dependent freezing behaviour in immersion mode ice nucleation, Atmos. Chem. Phys., 14, 8501–8520, https://doi.org/10.5194/acp-14-8501-2014, 2014.

Hiranuma, N., Adachi, K., Bell, D. M., Belosi, F., Beydoun, H., Bhaduri, B., Bingemer, H., Budke, C., Clemen, H.-C., Conen, F., Cory, K. M., Curtius, J., DeMott, P. J., Eppers, O., Grawe, S., Hartmann, S., Hoffmann, N., Höhler, K., Jantsch, E., Kiselev, A., Koop, T., Kulkarni, G., Mayer, A., Murakami, M., Murray, B. J., Nicosia, A., Petters, M. D., Piazza, M., Polen, M., Reicher, N., Rudich, Y., Saito, A., Santachiara, G., Schiebel, T., Schill, G. P., Schneider, J., Segev, L., Stopelli, E., Sullivan, R. C., Suski, K., Szakáll, M., Tajiri, T., Taylor, H., Tobo, Y., Ullrich, R., Weber, D., Wex, H., Whale, T. F., Whiteside, C. L., Yamashita, K., Zelenyuk, A., and Möhler, O.: A comprehensive characterization of ice nucleation by three different types of cellulose particles immersed in water, Atmos. Chem. Phys., 19, 4823–4849, https://doi.org/10.5194/acp-19-4823-2019, 2019.

Hoose, C. and Möhler, O.: Heterogeneous ice nucleation on atmospheric aerosols: a review of results from laboratory experiments, Atmos. Chem. Phys., 12, 9817–9854, https://doi.org/10.5194/acp-12-9817-2012, 2012.

Huang, W. T. K., Ickes, L., Tegen, I., Rinaldi, M., Ceburnis, D., and Lohmann, U.: Global relevance of marine organic aerosol as ice nucleating particles, Atmos. Chem. Phys., 18, 11423–11445, https://doi.org/10.5194/acp-18-11423-2018, 2018.

Ickes, L., Porter, G. C. E., Wagner, R., Adams, M. P., Bierbauer, S., Christiansen, S., Höhler, K., Schiebel, T., Ullrich, R., and Salter, M.: Dataset ice nucleating activity of Arctic sea surface microlayer samples and marine algal cultures, KITopen, https://doi.org/10.5445/IR/1000122595, 2020.

Intrieri, J. M., Fairall, C. W., Shupe, M. D., Persson, P. O. G., Andreas, E. L., Guest, P. S., and Moritz, R. E.: An annual cycle of Arctic surface cloud forcing at SHEBA, J. Geophys. Res.-Oceans, 107, 8039, https://doi.org/10.1029/2000JC000439, 2002.

Irish, V. E., Elizondo, P., Chen, J., Chou, C., Charette, J., Lizotte, M., Ladino, L. A., Wilson, T. W., Gosselin, M., Murray, B. J., Polishchuk, E., Abbatt, J. P. D., Miller, L. A., and Bertram, A. K.: Ice-nucleating particles in Canadian Arctic sea-surface microlayer and bulk seawater, Atmos. Chem. Phys., 17, 10583–10595, https://doi.org/10.5194/acp-17-10583-2017, 2017.

Irish, V. E., Hanna, S. J., Willis, M. D., China, S., Thomas, J. L., Wentzell, J. J. B., Cirisan, A., Si, M., Leaitch, W. R., Murphy, J. G., Abbatt, J. P. D., Laskin, A., Girard, E., and Bertram, A. K.: Ice nucleating particles in the marine boundary layer in the Canadian Arctic during summer 2014, Atmos. Chem. Phys., 19, 1027–1039, https://doi.org/10.5194/acp-19-1027-2019, 2019a.

Irish, V. E., Hanna, S. J., Xi, Y., Boyer, M., Polishchuk, E., Ahmed, M., Chen, J., Abbatt, J. P. D., Gosselin, M., Chang, R., Miller, L. A., and Bertram, A. K.: Revisiting properties and concentrations of ice-nucleating particles in the sea surface microlayer and bulk seawater in the Canadian Arctic during summer, Atmos. Chem. Phys., 19, 7775–7787, https://doi.org/10.5194/acp-19-7775-2019, 2019b.

Isono, K., Komabayasi, M., and Ono, A.: The Nature and the Origin of Ice Nuclei in the. Atmosphere, J. Meteorol. Soc. Jpn. Ser. II, 37, 211–233, 1959.

Kanji, Z. A., Ladino, L. A., Wex, H., Boose, Y., Burkert-Kohn, M., Cziczo, D. J., and Krämer, M.: Overview of Ice Nucleating Particles, Meteor. Mon., 58, 1.1–1.33, https://doi.org/10.1175/AMSMONOGRAPHS-D-16-0006.1, 2017.

King, S. M., Butcher, A. C., Rosenoern, T., Coz, E., Lieke, K. I., de Leeuw, G., Nilsson, E. D., and Bilde, M.: Investigating Primary Marine Aerosol Properties: CCN Activity of Sea Salt and Mixed Inorganic–Organic Particles, Environ. Sci. Technol., 46, 10405–10412, https://doi.org/10.1021/es300574u, 2012.

Kline, D. B.: Recent Observations of Freezing Nuclei Variations at Ground Level, 240–246, American Geophysical Union (AGU), https://doi.org/10.1029/GM005p0240, 1960.

Kline, D. B. and Brier, G. W.: A note on freezing nuclei anomalies, Mon. Weather Rev., 86, 329–333, https://doi.org/10.1175/1520-0493(1958)086<0329:ANOFNA>2.0.CO;2, 1958.

Knopf, D. A., Alpert, P. A., Wang, B., and Aller, J. Y.: Stimulation of ice nucleation by marine diatoms, Nat. Geosci., 4, 88–90, https://doi.org/10.1038/ngeo1037, 2011.

Knulst, J. C., Rosenberger, D., Thompson, B., and Paatero, J.: Intensive Sea Surface Microlayer Investigations of Open Leads in

the Pack Ice during Arctic Ocean 2001 Expedition, Langmuir, 19, 10194–10199, https://doi.org/10.1021/la035069+, 2003.

Kooistra, W. H., Sarno, D., Balzano, S., Gu, H., Andersen, R. A., and Zingone, A.: Global Diversity and Biogeography of Skeletonema Species (Bacillariophyta), Protist, 159, 177–193, https://doi.org/10.1016/j.protis.2007.09.004, 2008.

Koop, T., Kapilashrami, A., Molina, L. T., and Molina, M. J.: Phase transitions of sea-salt/water mixtures at low temperatures: Implications for ozone chemistry in the polar marine boundary layer, J. Geophys. Res.-Atmos., 105, 26393–26402, https://doi.org/10.1029/2000JD900413, 2000.

Ladino, L. A., Yakobi-Hancock, J. D., Kilthau, W. P., Mason, R. H., Si, M., Li, J., Miller, L. A., Schiller, C. L., Huffman, J. A., Aller, J. Y., Knopf, D. A., Bertram, A. K., and Abbatt, J. P. D.: Addressing the ice nucleating abilities of marine aerosol: A combination of deposition mode laboratory and field measurements, Atmos. Environ., 132, 1–10, https://doi.org/10.1016/j.atmosenv.2016.02.028, 2016.

Ladino, L. A., Raga, G. B., Alvarez-Ospina, H., Andino-Enríquez, M. A., Rosas, I., Martínez, L., Salinas, E., Miranda, J., Ramírez-Díaz, Z., Figueroa, B., Chou, C., Bertram, A. K., Quintana, E. T., Maldonado, L. A., García-Reynoso, A., Si, M., and Irish, V. E.: Ice-nucleating particles in a coastal tropical site, Atmos. Chem. Phys., 19, 6147–6165, https://doi.org/10.5194/acp-19-6147-2019, 2019.

Langer, G. and Rodgers, J.: An Experimental Study of the Detection of Ice Nuclei on Membrane Filters and Other Substrata, J. Appl. Meteorol., 14, 560–570, https://doi.org/10.1175/1520-0450(1975)014<0560:AESOTD>2.0.CO;2, 1975.

Langer, G., Rosinski, J., and Edwards, C. P.: A Continuous Ice Nucleus Counter and its Application to Tracking in the Troposphere, J. Appl. Meteorol., 6, 114–125, https://doi.org/10.1175/1520-0450(1967)006<0114:ACINCA>2.0.CO;2, 1967.

Larsen, J. A., Conen, F., and Alewell, C.: Export of ice nucleating particles from a watershed, Roy. Soc. Open Sci., 4, 170213, https://doi.org/10.1098/rsos.170213, 2017.

Leck, C., Norman, M., Bigg, E. K., and Hillamo, R.: Chemical composition and sources of the high Arctic aerosol relevant for cloud formation, J. Geophys. Res.-Atmos., 107, AAC 1-1–AAC 1-17, https://doi.org/10.1029/2001JD001463, 2002.

Maki, L. R., Galyan, E. L., Chang-Chien, M.-M., and Caldwell, D. R.: Ice nucleation induced by Pseudomonas syringae, Appl. Environ. Microbiol., 28, 456–459, 1974.

Mason, R. H., Si, M., Li, J., Chou, C., Dickie, R., Toom-Sauntry, D., Pöhlker, C., Yakobi-Hancock, J. D., Ladino, L. A., Jones, K., Leaitch, W. R., Schiller, C. L., Abbatt, J. P. D., Huffman, J. A., and Bertram, A. K.: Ice nucleating particles at a coastal marine boundary layer site: correlations with aerosol type and meteorological conditions, Atmos. Chem. Phys., 15, 12547–12566, https://doi.org/10.5194/acp-15-12547-2015, 2015.

Matrai, P. A., Tranvik, L., Leck, C., and Knulst, J. C.: Are high Arctic surface microlayers a potential source of aerosol organic precursors?, Mar. Chem., 108, 109–122, https://doi.org/10.1016/j.marchem.2007.11.001, 2008.

McCluskey, C. S., Hill, T. C. J., Malfatti, F., Sultana, C. M., Lee, C., Santander, M. V., Beall, C. M., Moore, K. A., Cornwell, G. C., Collins, D. B., Prather, K. A., Jayarathne, T., Stone, E. A., Azam, F., Kreidenweis, S. M., and DeMott, P. J.: A Dynamic Link between Ice Nucleating Particles Released in Nascent Sea Spray Aerosol and Oceanic Biological Activity during Two Mesocosm Experiments, J. Atmos. Sci., 74, 151–166, https://doi.org/10.1175/JAS-D-16-0087.1, 2017.

McCluskey, C. S., Hill, T. C. J., Humphries, R. S., Rauker, A. M., Moreau, S., Strutton, P. G., Chambers, S. D., Williams, A. G., McRobert, I., Ward, J., Keywood, M. D., Harnwell, J., Ponsonby, W., Loh, Z. M., Krummel, P. B., Protat, A., Kreidenweis, S. M., and DeMott, P. J.: Observations of Ice Nucleating Particles Over Southern Ocean Waters, Geophys. Res. Lett., 45, 11989–11997, https://doi.org/10.1029/2018GL079981, 2018a.

McCluskey, C. S., Ovadnevaite, J., Rinaldi, M., Atkinson, J., Belosi, F., Ceburnis, D., Marullo, S., Hill, T. C. J., Lohmann, U., Kanji, Z. A., O'Dowd, C., Kreidenweis, S. M., and DeMott, P. J.: Marine and Terrestrial Organic Ice-Nucleating Particles in Pristine Marine to Continentally Influenced Northeast Atlantic Air Masses, J. Geophys. Res.-Atmos., 123, 6196–6212, https://doi.org/10.1029/2017JD028033, 2018b.

Moffett, B., Hill, T., and DeMott, P.: Abundance of biological ice nucleating particles in the Mississippi and its major tributaries, Atmosphere, 9, 307, https://doi.org/10.3390/atmos9080307, 2018.

Möhler, O., Stetzer, O., Schaefers, S., Linke, C., Schnaiter, M., Tiede, R., Saathoff, H., Krämer, M., Mangold, A., Budz, P., Zink, P., Schreiner, J., Mauersberger, K., Haag, W., Kärcher, B., and Schurath, U.: Experimental investigation of homogeneous freezing of sulphuric acid particles in the aerosol chamber AIDA, Atmos. Chem. Phys., 3, 211–223, https://doi.org/10.5194/acp-3-211-2003, 2003.

Möhler, O., Büttner, S., Linke, C., Schnaiter, M., Saathoff, H., Stetzer, O., Wagner, R., Krämer, M., Mangold, A., Ebert, V., and Schurath, U.: Effect of sulfuric acid coating on heterogeneous ice nucleation by soot aerosol particles, J. Geophys. Res.-Atmos., 110, D11210, https://doi.org/10.1029/2004JD005169, 2005.

Möhler, O., Benz, S., Saathoff, H., Schnaiter, M., Wagner, R., Schneider, J., Walter, S., Ebert, V., and Wagner, S.: The effect of organic coating on the heterogeneous ice nucleation efficiency of mineral dust aerosols, Environ. Res. Lett., 3, 025007, https://doi.org/10.1088/1748-9326/3/2/025007, 2008.

Morrison, H., de Boer, G., Feingold, G., Harrington, J., Shupe, M. D., and Sulia, K.: Resilience of persistent Arctic mixed-phase clouds, Nat. Geosci., 5, 11–17, 2012.

Murphy, D. M. and Koop, T.: Review of the vapour pressures of ice and supercooled water for atmospheric applications, Q. J. Roy. Meteor. Soc., 131, 1539–1565, https://doi.org/10.1256/qj.04.94, 2005.

Murray, B. J., O'Sullivan, D., Atkinson, J. D., and Webb, M. E.: Ice nucleation by particles immersed in supercooled cloud droplets, Chem. Soc. Rev., 41, 6519–6554, https://doi.org/10.1039/C2CS35200A, 2012.

Nagamoto, C. T., Rosinski, J., Haagenson, P. L., Michalowska-Smak, A., and Parungo, F.: Characteristics of ice-forming nuclei in continental-maritime air, J. Aerosol Sci., 15, 147–166, 1984.

Niemand, M., Möhler, O., Vogel, B., Vogel, H., Hoose, C., Connolly, P., Klein, H., Bingemer, H., DeMott, P., Skrotzki, J., and Leisner, T.: A Particle-Surface-Area-Based Parameterization of Immersion Freezing on Desert Dust Particles, J. Atmos. Sci., 69, 3077–3092, https://doi.org/10.1175/JAS-D-11-0249.1, 2012.

O'Dowd, C. D., Facchini, M. C., Cavalli, F., Ceburnis, D., Mircea, M., Decesari, S., Fuzzi, S., Yoon, Y. J., and Putaud, J.-P.: Bio-

genically driven organic contribution to marine aerosol, Nature, 431, 676–680, https://doi.org/10.1038/nature02959, 2004.

Orellana, M. V., Matrai, P. A., Leck, C., Rauschenberg, C. D., Lee, A. M., and Coz, E.: Marine microgels as a source of cloud condensation nuclei in the high Arctic, P. Natl. Acad. Sci. USA, 108, 13612–13617, https://doi.org/10.1073/pnas.1102457108, 2011.

O'Sullivan, D., Murray, B. J., Malkin, T. L., Whale, T. F., Umo, N. S., Atkinson, J. D., Price, H. C., Baustian, K. J., Browse, J., and Webb, M. E.: Ice nucleation by fertile soil dusts: relative importance of mineral and biogenic components, Atmos. Chem. Phys., 14, 1853–1867, https://doi.org/10.5194/acp-14-1853-2014, 2014.

O'Sullivan, D., Murray, B. J., Ross, J. F., Whale, T. F., Price, H. C., Atkinson, J. D., Umo, N. S., and Webb, M. E.: The relevance of nanoscale biological fragments for ice nucleation in clouds, Sci. Rep.-UK, 5, 8082, https://doi.org/10.1038/srep08082, 2015.

O'Sullivan, D., Murray, B. J., Ross, J. F., and Webb, M. E.: The adsorption of fungal ice-nucleating proteins on mineral dusts: a terrestrial reservoir of atmospheric ice-nucleating particles, Atmos. Chem. Phys., 16, 7879–7887, https://doi.org/10.5194/acp-16-7879-2016, 2016.

Parker, L. V., Sullivan, C. W., Forest, T. W., and Ackley, S. F.: Ice nucleation activity of Antarctic marine microorganisms, Antarctic J., 20, 126–127, 1985.

Phelps, P., Giddings, T. H., Prochoda, M., and Fall, R.: Release of cell-free ice nuclei by Erwinia herbicola, J. Bacteriol., 167, 496–502, 1986.

Pithan, F. and Mauritsen, T.: Arctic amplification dominated by temperature feedbacks in contemporary climate models, Nat. Geosci., 7, 181–184, 2014.

Polen, M., Lawlis, E., and Sullivan, R. C.: The unstable ice nucleation properties of Snomax® bacterial particles, J. Geophys. Res.-Atmos., 121, 11666–11678, https://doi.org/10.1002/2016JD025251, 2016.

Pouleur, S., Richard, C., Martin, J.-G., and Antoun, H.: Ice Nucleation Activity in Fusarium acuminatum and Fusarium avenaceum, Appl. Environ. Microb., 58, 2960–2964, 1992.

Prather, K. A., Bertram, T. H., Grassian, V. H., Deane, G. B., Stokes, M. D., DeMott, P. J., Aluwihare, L. I., Palenik, B. P., Azam, F., Seinfeld, J. H., Moffet, R. C., Molina, M. J., Cappa, C. D., Geiger, F. M., Roberts, G. C., Russell, L. M., Ault, A. P., Baltrusaitis, J., Collins, D. B., Corrigan, C. E., Cuadra-Rodriguez, L. A., Ebben, C. J., Forestieri, S. D., Guasco, T. L., Hersey, S. P., Kim, M. J., Lambert, W. F., Modini, R. L., Mui, W., Pedler, B. E., Ruppel, M. J., Ryder, O. S., Schoepp, N. G., Sullivan, R. C., and Zhao, D.: Bringing the ocean into the laboratory to probe the chemical complexity of sea spray aerosol, P. Natl. Acad. Sci. USA, 110, 7550–7555, https://doi.org/10.1073/pnas.1300262110, 2013.

Radke, L. F., Hobbs, P. V., and Pinnons, J. E.: Observations of Cloud Condensation Nuclei, Sodium-Containing Particles, Ice Nuclei and the Light-Scattering Coefficient Near Barrow, Alaska, J. Appl. Meteorol., 15, 982–995, https://doi.org/10.1175/1520-0450(1976)015<0982:OOCCNS>2.0.CO;2, 1976.

Rogers, D. C.: Development of a continuous flow thermal gradient diffusion chamber for ice nucleation studies, Atmos. Res., 22, 149–181, https://doi.org/10.1016/0169-8095(88)90005-1, 1988.

Rosinski, J.: Cloud condensation nuclei as a real source of ice forming nuclei in continental and marine air masses, Atmos. Res., 38, 351–359, 1995.

Rosinski, J., Haagenson, P. L., Nagamoto, C. T., and Parungo, F.: Ice-forming nuclei of maritime origin, J. Aerosol Sci., 17, 23–46, https://doi.org/10.1016/0021-8502(86)90004-2, 1986.

Rosinski, J., Haagenson, P. L., Nagamoto, C. T., and Parungo, F.: Nature of ice-forming nuclei in marine air masses, J. Aerosol Sci., 18, 291–309, 1987.

Rosinski, J., Haagenson, P., Nagamoto, C., Quintana, B., Parungo, F., and Hoyt, S.: Ice-forming nuclei in air masses over the Gulf of Mexico, J. Aerosol Sci., 19, 539–551, https://doi.org/10.1016/0021-8502(88)90206-6, 1988.

Rosinski, J., Nagamoto, C. T., and Zhou, M. Y.: Ice-forming nuclei over the East China Sea, Atmos. Res., 36, 95–105, 1995.

Saravanan, V. and Godhe, A.: Genetic heterogeneity and physiological variation among seasonally separated clones of Skeletonema marinoi (Bacillariophyceae) in the Gullmar Fjord, Sweden, Eur. J. Phycol., 45, 177–190, https://doi.org/10.1080/09670260903445146, 2010.

Schiebel, T.: Ice Nucleation Activity of Soil Dust Aerosols, PhD thesis, Karlsruher Institut für Technologie (KIT), https://doi.org/10.5445/IR/1000076327, LK 01, 2017.

Schnell, R. C.: Ice nuclei produced by laboratory cultured marine phytoplankton, Geophys. Res. Lett., 2, 500–502, 1975.

Schnell, R. C.: Ice Nuclei in Seawater, Fog Water and Marine Air off the Coast of Nova Scotia: Summer 1975, J. Atmos. Sci., 34, 1299–1305, https://doi.org/10.1175/1520-0469(1977)034<1299:INISFW>2.0.CO;2, 1977.

Schnell, R. C. and Vali, G.: Freezing nuclei in marine waters, Tellus, 27, 321–323, https://doi.org/10.1111/j.2153-3490.1975.tb01682.x, 1975.

Schnell, R. C. and Vali, G.: Biogenic Ice Nuclei: Part I. Terrestrial and Marine Sources, J. Atmos. Sci., 33, 1554–1564, https://doi.org/10.1175/1520-0469(1976)033<1554:BINPIT>2.0.CO;2, 1976.

Shinki, M., Wendeberg, M., Vagle, S., Cullen, J. T., and Hore, D. K.: Characterization of adsorbed microlayer thickness on an oceanic glass plate sampler, Limnol. Oceanogr.-Meth., 10, 728–735, https://doi.org/10.4319/lom.2012.10.728, 2012.

Shupe, M. D., Matrosov, S. Y., and Uttal, T.: Arctic Mixed-Phase Cloud Properties Derived from Surface-Based Sensors at SHEBA, J. Atmos. Sci., 63, 697–711, https://doi.org/10.1175/JAS3659.1, 2006.

Si, M., Irish, V. E., Mason, R. H., Vergara-Temprado, J., Hanna, S. J., Ladino, L. A., Yakobi-Hancock, J. D., Schiller, C. L., Wentzell, J. J. B., Abbatt, J. P. D., Carslaw, K. S., Murray, B. J., and Bertram, A. K.: Ice-nucleating ability of aerosol particles and possible sources at three coastal marine sites, Atmos. Chem. Phys., 18, 15669–15685, https://doi.org/10.5194/acp-18-15669-2018, 2018.

Si, M., Evoy, E., Yun, J., Xi, Y., Hanna, S. J., Chivulescu, A., Rawlings, K., Veber, D., Platt, A., Kunkel, D., Hoor, P., Sharma, S., Leaitch, W. R., and Bertram, A. K.: Concentrations, composition, and sources of ice-nucleating particles in the Canadian High Arctic during spring 2016, Atmos. Chem. Phys., 19, 3007–3024, https://doi.org/10.5194/acp-19-3007-2019, 2019.

Stevenson, C. M.: An improved Millipore filter technique for measuring the concentrations of freezing nuclei in the atmosphere, Q. J. Roy. Meteor. Soc., 94, 35–43, 1968.

Stocker, T. F., Qin, D., Plattner, G.-K., Tignor, M., Allen, S. K., Boschung, J., Nauels, A., Xia, Y., Bex, V., and Midgley, P. M.: Climate Change 2013: The Physical Science Basis. Contribution of Working Group I to the Fifth Assessment Report of the Intergovernmental Panel on Climate Change, Cambridge University Press, 2013.

Suikkanen, S., Hakanen, P., Spilling, K., and Kremp, A.: Allelopathic effects of Baltic Sea spring bloom dinoflagellates on co-occurring phytoplankton, Mar. Ecol.-Prog. Ser., 439, 45–55, https://doi.org/10.3354/meps09356, 2011.

Suski, K. J., Hill, T. C. J., Levin, E. J. T., Miller, A., DeMott, P. J., and Kreidenweis, S. M.: Agricultural harvesting emissions of ice-nucleating particles, Atmos. Chem. Phys., 18, 13755–13771, https://doi.org/10.5194/acp-18-13755-2018, 2018.

Szyrmer, W. and Zawadzki, I.: Biogenic and anthropogenic sources of ice-forming nuclei: A review, B. Am. Meteorol. Soc., 78, 209–228, 1997.

Tang, I. N., Tridico, A. C., and Fung, K. H.: Thermodynamic and optical properties of sea salt aerosols, J. Geophys. Res.-Atmos., 102, 23269–23275, https://doi.org/10.1029/97JD01806, 1997.

Tesson, S. V. M. and Šantl Temkiv, T.: Ice Nucleation Activity and Aeolian Dispersal Success in Airborne and Aquatic Microalgae, Front. Microbiol., 9, 2681, https://doi.org/10.3389/fmicb.2018.02681, 2018.

Tjernström, M., Leck, C., Birch, C. E., Bottenheim, J. W., Brooks, B. J., Brooks, I. M., Bäcklin, L., Chang, R. Y.-W., de Leeuw, G., Di Liberto, L., de la Rosa, S., Granath, E., Graus, M., Hansel, A., Heintzenberg, J., Held, A., Hind, A., Johnston, P., Knulst, J., Martin, M., Matrai, P. A., Mauritsen, T., Müller, M., Norris, S. J., Orellana, M. V., Orsini, D. A., Paatero, J., Persson, P. O. G., Gao, Q., Rauschenberg, C., Ristovski, Z., Sedlar, J., Shupe, M. D., Sierau, B., Sirevaag, A., Sjogren, S., Stetzer, O., Swietlicki, E., Szczodrak, M., Vaattovaara, P., Wahlberg, N., Westberg, M., and Wheeler, C. R.: The Arctic Summer Cloud Ocean Study (ASCOS): overview and experimental design, Atmos. Chem. Phys., 14, 2823–2869, https://doi.org/10.5194/acp-14-2823-2014, 2014.

Ullrich, R., Hoose, C., Möhler, O., Niemand, M., Wagner, R., Höhler, K., Hiranuma, N., Saathoff, H., and Leisner, T.: A New Ice Nucleation Active Site Parameterization for Desert Dust and Soot, J. Atmos. Sci., 74, 699–717, https://doi.org/10.1175/JAS-D-16-0074.1, 2017.

Vali, G.: Quantitative evaluation of experimental results an the heterogeneous freezing nucleation of supercooled liquids, J. Atmos. Sci., 28, 402–409, 1971.

Vali, G.: Atmospheric ice nucleation–A review, J. Rech. Atmos., 19, 105–115, 1985.

Vali, G., Christensen, M., Fresh, R. W., Galyan, E. L., Maki, L. R., and Schnell, R. C.: Biogenic ice nuclei. Part II: Bacterial sources, J. Atmos. Sci., 33, 1565–1570, 1976.

Vali, G., DeMott, P. J., Möhler, O., and Whale, T. F.: Technical Note: A proposal for ice nucleation terminology, Atmos. Chem. Phys., 15, 10263–10270, https://doi.org/10.5194/acp-15-10263-2015, 2015.

Vergara-Temprado, J., Murray, B. J., Wilson, T. W., O'Sullivan, D., Browse, J., Pringle, K. J., Ardon-Dryer, K., Bertram, A. K., Burrows, S. M., Ceburnis, D., DeMott, P. J., Mason, R. H., O'Dowd, C. D., Rinaldi, M., and Carslaw, K. S.: Contribution of feldspar and marine organic aerosols to global ice nucleating particle concentrations, Atmos. Chem. Phys., 17, 3637–3658, https://doi.org/10.5194/acp-17-3637-2017, 2017.

Wagner, R. and Möhler, O.: Heterogeneous ice nucleation ability of crystalline sodium chloride dihydrate particles, J. Geophys. Res.-Atmos., 118, 4610–4622, https://doi.org/10.1002/jgrd.50325, 2013.

Wang, X., Sultana, C. M., Trueblood, J., Hill, T. C. J., Malfatti, F., Lee, C., Laskina, O., Moore, K. A., Beall, C. M., McCluskey, C. S., Cornwell, G. C., Zhou, Y., Cox, J. L., Pendergraft, M. A., Santander, M. V., Bertram, T. H., Cappa, C. D., Azam, F., DeMott, P. J., Grassian, V. H., and Prather, K. A.: Microbial Control of Sea Spray Aerosol Composition: A Tale of Two Blooms, ACS Central Science, 1, 124–131, https://doi.org/10.1021/acscentsci.5b00148, 2015.

Warner, J.: An instrument for the measurement of freezing nucleus concentration, Bulletin de L'Observatoire du Puy de Dome, 2, 33–46, 1957.

Welti, A., Müller, K., Fleming, Z. L., and Stratmann, F.: Concentration and variability of ice nuclei in the subtropical maritime boundary layer, Atmos. Chem. Phys., 18, 5307–5320, https://doi.org/10.5194/acp-18-5307-2018, 2018.

Welti, A., Bigg, E. K., DeMott, P. J., Gong, X., Hartmann, M., Harvey, M., Henning, S., Herenz, P., Hill, T. C. J., Hornblow, B., Leck, C., Löffler, M., McCluskey, C. S., Rauker, A. M., Schmale, J., Tatzelt, C., van Pinxteren, M., and Stratmann, F.: Ship-based measurements of ice nuclei concentrations over the Arctic, Atlantic, Pacific and Southern Ocean, Atmos. Chem. Phys. Discuss., https://doi.org/10.5194/acp-2020-466, in review, 2020.

Wex, H., Huang, L., Zhang, W., Hung, H., Traversi, R., Becagli, S., Sheesley, R. J., Moffett, C. E., Barrett, T. E., Bossi, R., Skov, H., Hünerbein, A., Lubitz, J., Löffler, M., Linke, O., Hartmann, M., Herenz, P., and Stratmann, F.: Annual variability of ice-nucleating particle concentrations at different Arctic locations, Atmos. Chem. Phys., 19, 5293–5311, https://doi.org/10.5194/acp-19-5293-2019, 2019.

Whale, T. F., Murray, B. J., O'Sullivan, D., Wilson, T. W., Umo, N. S., Baustian, K. J., Atkinson, J. D., Workneh, D. A., and Morris, G. J.: A technique for quantifying heterogeneous ice nucleation in microlitre supercooled water droplets, Atmos. Meas. Tech., 8, 2437–2447, https://doi.org/10.5194/amt-8-2437-2015, 2015.

Wilbourn, E. K., Thornton, D. C. O., Ott, C., Graff, J., Quinn, P. K., Bates, T. S., Betha, R., Russell, L. M., Behrenfeld, M. J., and Brooks, S. D.: Ice Nucleation by Marine Aerosols Over the North Atlantic Ocean in Late Spring, J. Geophys. Res.-Atmos., 125, e2019JD030913, https://doi.org/10.1029/2019JD030913, 2020.

Willis, M. D., Leaitch, W. R., and Abbatt, J. P.: Processes Controlling the Composition and Abundance of Arctic Aerosol, Rev. Geophys., 56, 621–671, https://doi.org/10.1029/2018RG000602, 2018.

Wilson, T. W., Ladino, L. A., Alpert, P. A., Breckels, M. N., Brooks, I. M., Browse, J., Burrows, S. M., Carslaw, K. S., Huffman, J. A., Judd, C., Kilthau, W. P., Mason, R. H., McFiggans, G., Miller, L. A., Najera, J. J., Polishchuk, E., Rae, S., Schiller, C. L., Si, M., Temprado, J. V., Whale, T. F., Wong, J. P. S., Wurl, O., Yakobi-Hancock, J. D., Abbatt, J. P. D., Aller, J. Y., Bertram, A. K., Knopf, D. A., and Murray, B. J.: A marine biogenic source

of atmospheric ice-nucleating particles, Nature, 525, 234–238, https://doi.org/10.1038/nature14986, 2015.

Wolf, M. J., Goodell, M., Dong, E., Dove, L. A., Zhang, C., Franco, L. J., Shen, C., Rutkowski, E. G., Narducci, D. N., Mullen, S., Babbin, A. R., and Cziczo, D. J.: A Link between the Ice Nucleation Activity of Sea Spray Aerosol and the Biogeochemistry of Seawater, Atmos. Chem. Phys. Discuss., https://doi.org/10.5194/acp-2020-416, in review, 2020.

Wright, T. P. and Petters, M. D.: The role of time in heterogeneous freezing nucleation, J. Geophys. Res.-Atmos., 118, 3731–3743, https://doi.org/10.1002/jgrd.50365, 2013.

Yun, Y. and Penner, J. E.: An evaluation of the potential radiative forcing and climatic impact of marine organic aerosols as heterogeneous ice nuclei, Geophys. Res. Lett., 40, 4121–4126, https://doi.org/10.1002/grl.50794, 2013.

Zieger, P., Väisänen, O., Corbin, J. C., Partridge, D. G., Bastelberger, S., Mousavi-Fard, M., Rosati, B., Gysel, M., Krieger, U. K., Leck, C., Nenes, A., Riipinen, I., Virtanen, A., and Salter, M. E.: Revising the hygroscopicity of inorganic sea salt particles, Nat. Commun., 8, 15883, https://doi.org/10.1038/ncomms15883, 2017.